

1. Aims and purposes of the satellite

The main mission objective of the micro satellite **Lunar ION ExploreR (LIONER)** is to perform a thorough investigation on the lunar ionosphere using the methods of the radio occultation (RO), in-situ measurement and remote sensing. Every terrestrial planet with an atmosphere has their own ionosphere which is a layer of ionized gas created by the solar ultraviolet rays acting on the atoms of air at the high altitude. Ionosphere plays an important role in our daily life. For example, the ionosphere reflects radio waves, allowing shortwave radio transmitter to bounce signals over the horizon for long-range communications. The ionosphere also bends and scatters signals from GPS satellites, sometimes causing GPS trackers to mis-read the correct positions.

The first convincing evidence for the existing of the lunar ionosphere came in the 1970s by the Soviet probes Luna 19 and 22 [Vyshlov,1976]. Orbiting the Moon at close range, the orbiters detected a layer of charged particles extending a few tens of km above the lunar surface containing as many as $10^3 \text{ e}^-/\text{cm}^3$ —a thousand times more than any theory could explain. Radio astronomers found another evidence: the distant radio sources passed behind the Moon's limb was bended and it hints the existence of the lunar ionosphere. On the other hand, there is hardly air on the Moon, only an extremely thin layer of gases on the lunar surface that can barely be called an atmosphere. Technically, it is considered as an exosphere. The idea of an "airless Moon" having an ionosphere doesn't make much sense, but the evidence seems compelling.

Therefore, some space probes undertook measurement toward the lunar ionosphere or atmosphere while flying by, or orbiting. Different from Earth's ionosphere, the lunar ionosphere isn't surrounding and protected by a magnetic field and the lunar gravity is much smaller than that of Earth. Therefore, the composition of the lunar ionosphere and their interactions with the solar wind is expected to be greatly different from the dynamic processes observed in the terrestrial ionosphere. Thus, the exploration of the lunar ionosphere can also help to evaluate its impact, especially under various conditions of the solar activities, on the communication between Earth, which is an important issue to establish a permanent base or immigration at the lunar surface in the foreseeable future. Therefore, scientists have been highly interested in the properties of the lunar ionosphere and atmosphere for a long time.

At first, the lunar ionosphere was expected to be formed by the photoionization of dilute air comprising argon (Ar) and helium (He). A theoretical model estimated that the dayside density of air was approximately $10^5 \text{ particles cm}^{-3}$. Assuming a spherical symmetry of the electron layer of the lunar ionosphere, the electron density of the ionosphere from the lunar surface to altitude of 100 km may remain only a few cm^{-3} . It was generally believed that the major physical process for producing such a low plasma density was driven by the convection electric field of the solar wind, and this electric field wiped ions away, preventing them from accumulating on the lunar surface. However, the RO measurements done by radio astronomers cannot agree with this model. Radio waves from the sources were found to be refracted significantly while the source was occulted by the dayside lunar limb. This occultation suggests the significant plasma existing above the lunar surface to forms the lunar ionosphere. With the bending angle, a revised model of the lunar ionosphere was proposed, in which the electron density in ionosphere is in the order of the magnitude around 1000 cm^{-3} [1].

To understand the discrepancy between the measured results and the current model, and also to investigate the origin of this airless ionosphere and its interaction as well as evolution with the solar activities, several spacecrafts were launched to study lunar ionosphere in the past decades [Wickert et al., 2007]. RO is one approach of the observations and it is now widely used in the exploration of ionosphere on Earth, such as CHAMP (2001~2008), GRACE (2002~2017), FORMOSAT-3/COSMIC (2016~present) and upcoming FORMOSAT-7/COSMIC-2. As shown in Fig. 1, the measurements with RO can obtain the vertical profiles of the plasma density of the planets or moons without in-situ measurement, and can be considered as an efficient way to explore the lunar ionosphere [2].

The total electron content (TEC) with respect to the altitude at this specific location can be obtained with RO which uses the bending angles and the phase shift of the radio waves emitted by one or many signal resources after the radio wave passing through the to-be measured ionosphere.

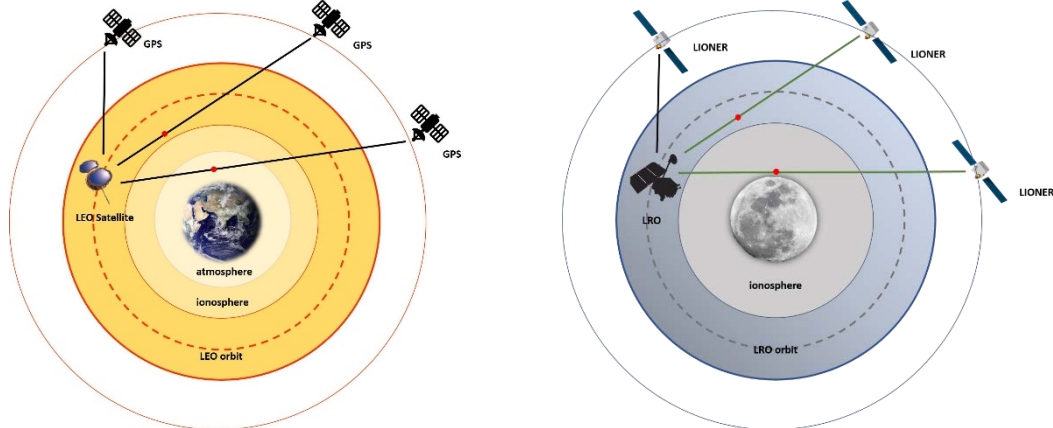


Figure 1. Concept of radio occultation, (left) the radio occultation assisted with GPS/GNSS as the signal emitter. (Right) a similar radio occultation proposed in this mission to measure the lunar ionosphere using NASA LRO at a lower orbit as the signal emitter. The green line represents a connection between LIONER and LRO to form a successful occultation, and the black line represents a fail one. The red dots on the green lines represent the place having a successful occultation data.

On the Moon, the first space probe performing RO was Pioneer 7 in 1966 [Pomalaza-Diaz,1967]. Its measurements confirmed the existence of the lunar ionosphere, and the measured electron density was approximately $10^2 \text{ e}^-/\text{cm}^3$. Afterwards, the following missions including Apollo 14, Selene (also known as Kaguya in Japan), Luna 19 and 22, also measured the lunar ionosphere using RO locally. Luna 19 and 22 from Soviet discovered a plasma layer with thickness of about 10 km and the electron density was $0.5\sim 10^3 \text{ e}^-/\text{cm}^3$. The columnar density of the ionosphere was estimated as $3\sim 5 \times 10^{14} \text{ e}^-/\text{cm}^2$. Furthermore, a remarkable variation between the electron density of the dayside and nightside was also found, and this measurement variation is not expected by any theoretical model at that time. On the other hand, RO done by SMART-1 gave a columnar density of $10^{13} \text{ e}^-/\text{cm}^2$, and the following Japanese Selene mission also yielded a similar result except that the difference of the electron density between dayside and nightside is not significant. The RO measurements by Indian Chandrayan-1 mission suggest that the lunar atmosphere consists of CO_2 , H_2O , HO , O , Ar , Ne , He and H_2 , in which CO_2 and H_2O are the major gases and the ratio of these two gases exceeds 50%. [3]

Beyond the ionosphere, the exosphere also receive great attentions, and missions such as Japanese PROCYON observed the geocorona which is formed the photons emitted from the exospheric hydrogen ions, i.e. proton, which is ionized by the solar ultraviolet radiation on the earth exosphere. For the Moon, a similar lunar corona of the ionized hydrogen and helium is also expected to be observed. Without the protection from a strong magnetic field, particles at the lunar surface can be easily perturbed by the Earth's gravity or solar wind and escape from the lunar surface. However, some particles can not gain sufficient energy to escape from moon's gravity to the vacuum space, therefore these particles surround the Moon, and form a corona under high energy solar irradiation. Since the exosphere and ionosphere are both affected by charged particles from sun, lunar corona will have deep relationship with the formation of ionosphere. Imaging lunar corona at the a carefully-selected band will thus give us a clearer picture about the interaction between the lunar ionosphere and solar wind [4].

When the Moon gets into magnetotail of Earth, its ionosphere and plasma environment can stretch in the dayside and darkside direction, and even is able to perturb nearby plasma coming from Sun or Earth. There may even exist a Moon-Earth plasma pathway, allowing two celestial bodies to exchange particles, and previous research from ARTEMIS suggested that such exchange do exists. However, such the existance of a plasma pathway and the meaning for Earth and Moon are still highly speculative issues for now. It is worth to mention that LIONER will have a good opportunity to detect

the change in the plasma environment when it passes through that region, and this will provide the confirmation of the hypothesis of the plasma pathway [4] [5].

Therefore, the LIONER mission is proposed to have a comprehensive investigation on the lunar ionosphere and is expected to achieve following goals:

- (1) To measure the vertical profiles of the ionospheric electron density by RO
- (2) To measure electron and ion density, and magnetic field of solar wind during interplanetary flight and at lunar orbit by in-situ measurement.
- (3) To observe lunar corona and geocorona by imaging at the hydrogen Lyman-alpha band.
- (4) To explore the formation and the dynamic processes of the lunar ionosphere and its association with the solar activities.

The conventional approach done by other spacecrafts used a terrestrial radio transmitter as the signal source in RO measurement, but the propagation distance of the signal exceeds 380,000 km and a powerful source is needed. Furthermore, the arrived signal at Moon can be easily perturbed by the earth ionosphere as well as the solar wind. Other than terrestrial radio sources, LIONER is designed to capture the radio wave emitted from existing lunar satellites, for example, the NASA LRO, or further spacecrafts orbiting the Moon with a S-band transmitter equipped instead of a terrestrial radio source to perform the RO measurements. With this approach, LIONER can avoid the contamination from the Earth ionosphere and the solar wind. The scientific payload of the LIONER consists of the S-band RO receiver, the ion and electron sensor (IES), Magnetometer (MAG), and Lyman Alpha Imaging Camera (LAICA). With the assistance of the naval technology - Solar Electric Propulsion (SEP), the fuel of this mission for the orbits transfer at the Earth after launch, cruising from the Earth to the Moon and orbiting insertion at Moon, can be greatly reduced. Therefore, more weight and space are able to be released for the scientific instruments. Using the SEP instead of the conventional chemistry propulsion will take a longer time from Earth to Moon, the detail will be shown and discussed in the later section. The whole mission is divided into seven phases: Earth orbit, GTO to Round orbit, Earth escaping, Cruising, Insertion, Circularize and Moon orbit. To have an in-deep exploration on the interaction between the solar wind and lunar ionosphere from the solar maximum to minimum activities, the best launch window is estimated after 2025. The time of the solar activity is expected to turn from quiet to active in 25th solar cycle (see Fig. 2) and the detail will be presented in the later section [6].

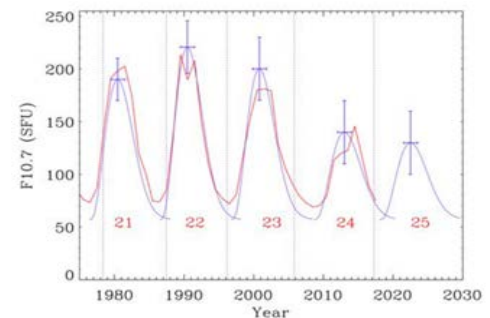


Figure 2. Solar activity predictions by Schatten et al., have used the polar magnetic field to predict 4 cycles and predict a low Cycle 25. The solar activity is expected to turn weaker after 2025, and reach to a solar minimum around 2030[6].

2. Design result

2.1.1. Orbital Analysis

The orbital design of the LIONER mission is to orbit the Moon at the altitude of 2,000 km with its own propulsion system from its first parking geostationary orbit lifted and placed by the H-IIA rocket. First, to reduce the fuel needed to reach the Moon, Solar Electric Propulsion (SEP), generally known as an ion propulsion, is considered as the propulsion system of the LIONER microsat. After surveying several commercial ion thrusters, the RIT 10 EVO [7] ion thruster is selected. However, the ion propulsion has very low thrust (the maximum thrust is 41 mN, and we will use only 15mN to ensure its reliability), the trajectory driven by the SEP is significantly different from the conventional

chemical propulsion with relatively large thrust but low specific impulse I_{sp} , or say energy efficiency. To demonstrate the feasibility of our mission, Astrogator, a tool for modeling and targeting orbit maneuver and spacecraft's trajectory, including impulsive and finite burns and high-fidelity orbit propagation and display it in a 2D or 3D animation, under STK [8] is used to perform the orbital design of the LIONER mission. During the design phase we also took the Electron and Power Subsystem (EPS) into consideration, i.e. we turn off the engine and wait for few hours to charge the battery before restarting the engine, making this trajectory more feasible. The design result is a 7-phase trajectory including Earth orbit, GTO to GEO, Earth escaping, Cruise, Insertion, Circularize and finally Moon orbit. Fig. 3 demonstrates the LIONER's trajectory to Moon from an Earth view.

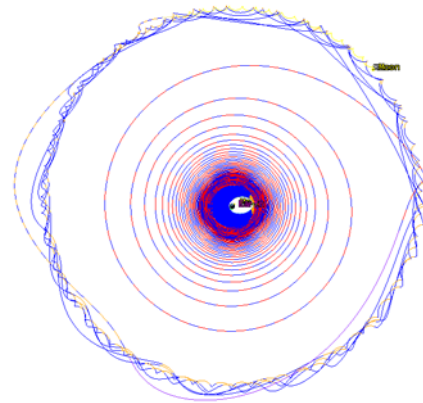


Figure 3. The whole trajectory of the LIONER microsat from launch to its arrival to Moon, Earth-centered view, propulsion and cruise (no thrust) of the spacecraft are marked with red and blue, respectively.

2.1.1.1. The Launch Window

To approach the Moon with a smaller inclination, we carefully select the launch window. The wrong departure date could result in high inclination insertion which could cause a polar orbit of moon and could change our ion detection range significantly. A good launch window can also reduce the required fuel for the orbit transfer. Since the angle between earth equatorial plane and ecliptic plane is 23.4° and the angle between lunar orbital inclination and ecliptic plane is 5.14° , so the different angle between two planes will be minimum value if LIONER's axis of rotation paralleled to the lunar orbital axis. Fortunately, the H-IIA rocket will launch in Japan where has an approximately 30° latitude. The positional relationship is shown in Fig.4 and this implies that **it is hardly change inclination** due to the orbital plane angle between

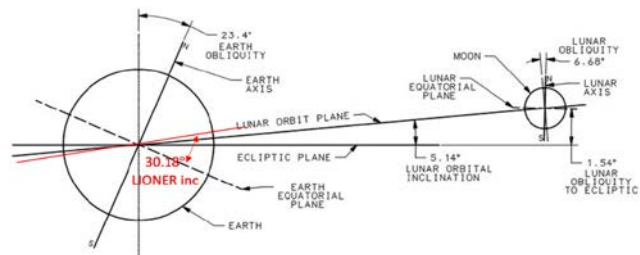


Figure 4. The positional relationship of LIONER , Moon and Earth[9]

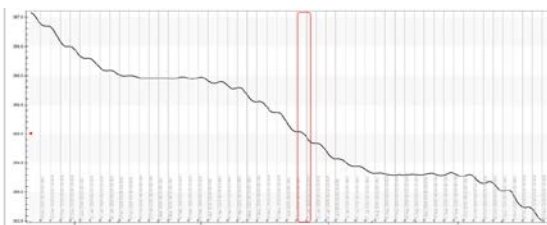


Figure 5. Lunsr RAAN respective to Earth in 2026

LIONER and Moon is 1.64° .

All we need is choosing the right launch window to lower difference between the angle plane. Therefore, we predict the time that LIONER will arrive to the Moon and the corresponding lunar right ascension of ascending node (RAAN) respect to Earth in Fig.5, i.e. LIONER's RAAN is preferably 355° , is 2026.

Tsiolkovsky rocket equation describes the motion of vehicles which follows the basic principle of a propulsion system, say LIONER:

$$\frac{\Delta m}{m} = 1 - e^{\frac{-\Delta V}{g \times I_{sp}}} \quad - (1)$$

Where m, V represent the mass and velocity of the LIONER microsat, respectively, therefore, $\Delta m, \Delta V$ indicate the change of mass and velocity, respectively. g is the gravitational acceleration on the surface of Earth or Moon, and I_{sp} is the specific impulse of the thruster. The equation implies that higher I_{sp} and lower ΔV can reduce Δm and save fuel.

To perform a Hohmann transfer [10] efficiently, Delta Burning is only triggered near the perilune. ΔV the velocity gained by delta burning without external force, is proportional to the consumed fuel, and is a good physical parameter to connect the calculation of the astrodynamics and fuel consumption. Assuming a fuel usage, the optimal launch window and possible mission elapse time for the LIONER microsat is iterated by the target sequence under STK, and a simple flow chart is presented in Fig. 6. Different fuel consumptions are calculated through the above process. With a lower fuel consumption or mission elapse time, the solutions of the accessible launch windows in the same evaluation period will be reduced or become impossible. Here the accessible launch windows in March 2025 is evaluated and demonstrated in Fig. 7. Only six launch windows are available in this month, and the best choice is 16th of March because the minimum of the ΔV , or fuel consumption occurs in this window. After taking at least 3.8 days of early Earth orbiting into account, the LIONER can have an optimal fuel usage if it launches from Tanegashima (latitude 30.4° North, longitude 130.97° East) before 12th of March 2025 and turns on the thruster on 16th March. The trajectories of other launch windows are also shown in Fig. 7.

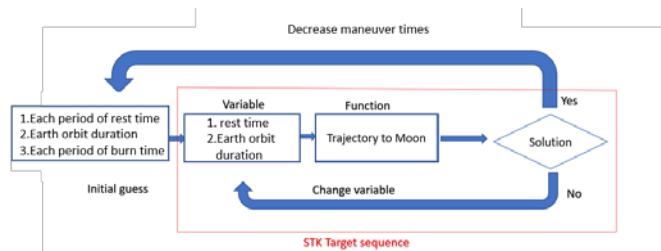


Figure 6. The iteration flow of the fuel and launch window

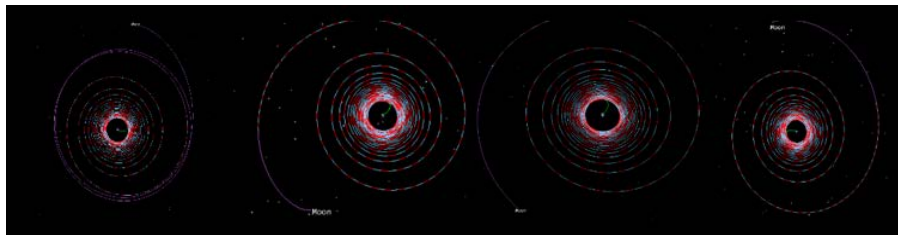


Figure 7. Iteration result of the optimal launch window. With an assumed V , the possible launch time and mission elapse time are iterated to evaluate the best launch window. The trajectories of launch window on 5th, 14th, 19th, 26th March are shown from left to right, respectively. Green line represents launch section, red line represents maneuver section, blue line represents the cruising section in the Earth center view.

2.1.1.2. Mission Phase

As mention on the previously section, the whole mission from launch to moon orbiting is divided into seven phases, including Earth orbit phase, GTO to Round orbit phase, Earth escaping phase, Insertion phase, Circularize phase, Mission orbiting phase as shown in Fig. 8, and each phase will be briefed below.

Earth orbit phase:

In this mission, the Japanese H-IIA rocket will be used as the launch vehicle and deliver the LIONER microsat to a Geostationary Transfer Orbit (GTO). In this parking orbit, the LIONER will perform early orbit check, then maneuver to a Round orbit at about 35,786 km above

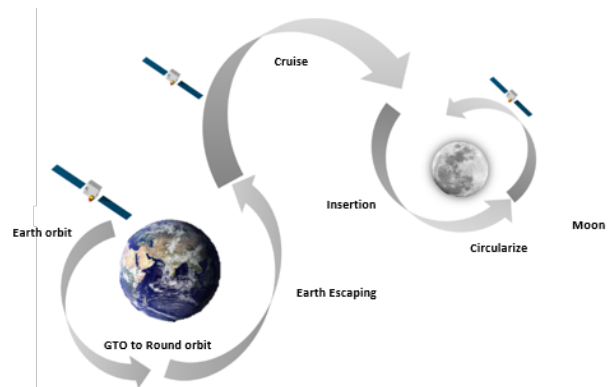


Figure 8. The sketch of the different phases of trajectory in the LIONER's mission

sea level, and the eccentricity of that orbit is assumed be 0. All subsystems and scientific payload will be inspected carefully during this phase.

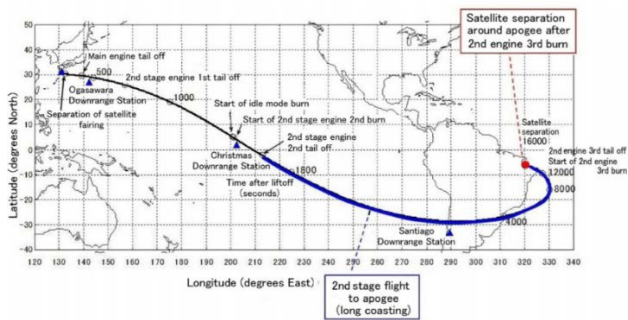


Figure 9. Trajectory of GTO long coasting mission [11]

GTO to Round orbit phase:

The reason for the need of LIONER changing from GTO to Round orbit is that during this period LIONER will turn on its engine near the apoapsis of the Earth for 4 hours, i.e. 2 hours before and after the Earth apoapsis, and cruise in other part of the orbit to charge its battery until arriving at the Earth apoapsis again. Although accelerating only happens near the apoapsis, LIONER can arrive and circularize at the Round orbit in shortest time. After 9 months and 445 times of acceleration, LIONER will reach a nearly the Round orbit with semi major axis of 43930 km and eccentricity of 0.013. After arriving at the Round orbit, LIONER will restart the engine and enter into the Earth escaping phase.



Figure 10. The trajectory for transferring from the GTO to Round orbit (Orange and blue line indicate maneuver and cruise respectively)

Earth escaping phase:

In this phase, LIONER will turn on and off the engine for 4 hours and 4.5 hours, to propel itself to the Moon. During this phase, the best approach conditions are the following requirements: First, it has to be within the Sphere of Influence (SOI) of the Moon, about 66,200 km from the lunar center to be influenced by the lunar gravity; Second, its final eccentricity should be smaller than 1 for an elliptical orbit. Finally, we chose the approach condition of 20686.6 km and eccentricity of 0.6, and determined the transfer trajectory from the Earth to the Moon. At the end of the phase, LIONER will pass through the Moon for the first time and get the first glimpse of the Moon. After travelling for 6 months, LIONER will enter into the Insertion phase for deceleration.

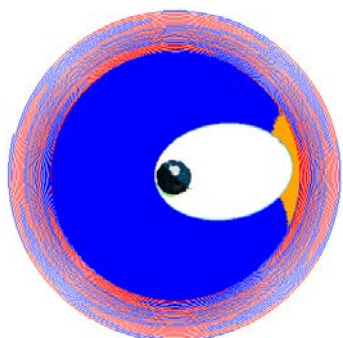


Figure 11. Earth escaping trajectory for 4/4.5 hour turn on /off the engine (Red and blue line indicate

Cruise phase:

After passing through the Moon, LIONER will turn off its ion engine for cruising. Being attracted by the lunar gravity, LIONER will then fly back to the Moon periapsis and have a 8- shape trajectory near the Moon. At the nearest part of the trajectory, LIONER will enter the region where gravitational pull from the Moon. In this phase LIONER will cruise to the Moon periapsis (or perilune) in 8 days as shown in Fig.12.

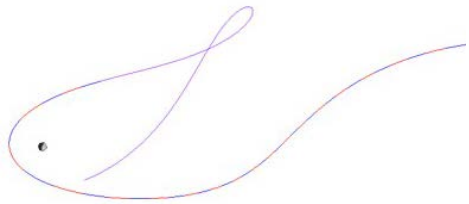


Figure 12. LIONER cruise to vicinity of the Moon and the purple line indicates the cruising period.

Insertion phase:

This is the most crucial phase in this mission, a life-or-death action. When the spacecraft approaches to the Moon, it must produce a ΔV to decrease its velocity (respect to the Moon), lower than the lunar escape velocity, and turns its hyperbolic or parabolic orbit into an elliptical one, i.e. insert LIONER into a lunar orbit.

To decelerate as fast as possible, LIONER will turn on its engine for 4 hours and shut it down for 4 hours before restarting the engine. After decelerating for 29 times, LIONER’s speed has been reduced to 0.255 km/s, well below the escape velocity at that altitude (0.49 km/s at 38,000 km altitude) with eccentricity of 0.9. After Insertion phase, LIONER cannot escape the Moon, but such high eccentricity means that it has to turn its orbit shape in to a more circular one, thus performing Circularize phase.

Circularize phase:

Just like the “GTO to Round orbit phase”, LIONER will circularize its orbit during this phase with deceleration instead of the acceration in the GTO to Round orbit. Therefore the maneuver point will be near periapsis of the Moon (perilune), Fig.14. Because of the effect of moon shadow on EPS system, the maneuver time will be reduced to 3 hours, i.e. 1.5 hours before and after perilune, to save power. After 5 months and 166 times of deceleration, LIONER will enter into moon orbit phase with semi major axis of 3,755 km (about 2000 km altitude) and eccentricity of 0.0016, almost circular orbit shown in Fig.15.

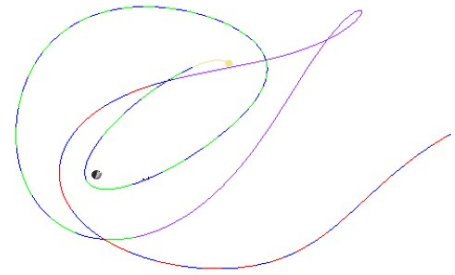


Figure 13. Trajectory of insertion and the green line indicates maneuver of the insertion phase

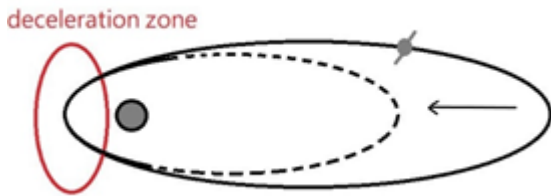


Figure 14. A series of continuous thrust are carried out at perilune to descend LIONER gradually into its lunar mission orbit with an altitude of 2,000 km.

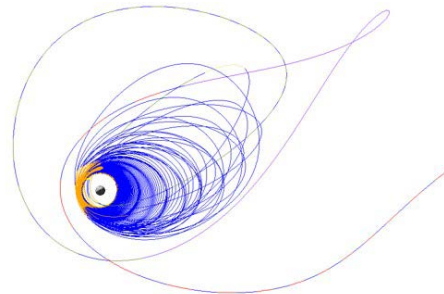


Figure 15. The trajectory of the insertion phase, moon-centered view, deacceleration and cruise (no thrust) of the spacecraft are marked with orange and blue, respectively.

Mission orbit phase:

After the insertion phase, LIONER reaches a Moon parking orbit with the orbit parameters listed in Table 1. It will stay there for mission operation and investigate ionosphere by all scientific payloads.

Table 1. Lunar orbit elements of the LIONER mission.

Classical Orbit Element of Moon Parking orbit			
Semimajor Axis (km)	3740.34	Inclination (deg)	20.76
Eccentricity	0.0017	RAAN (deg)	250.265
Argument of Periapsis(deg)	317.342	Mean Anomaly (deg)	340.84

The major orbital elements of these seven phases are summarized in Table 2, and all maneuver activities of LIONER are listed in Table 3. It is noted that there is no maneuver and fuel consumption during cruising, so the total duration of the cruising is not shown in this table.

Table 2. Summary of the LIONER orbits phases.

Phase	Coordinate	Semi-major axis (km)	Velocity (km/s)	C3 (km ² /s ²)	MET* (day)
Earth orbit	Earth	24,468	2.22	-16.29	3
GTO to Round orbit	Earth	43,930	3.053	-9.07	8 months
Earth escape	Earth	1,282,034	1.407	-0.31	6 months
Cruise	Moon	514,179	1.165	-0.77	8 days
Insertion	Moon	27,622	0.255	-0.177	10 days
Circularize	Moon	3,977	1.11	-1.232	4 months
Moon orbit	Moon	3,740	1.14	-1.31	2 years

*MET: Mission elapse time

Table 3. Maneuver time, duration and used fuel. There is no maneuver and fuel consumption during cruise, therefore the total duration of the cruise is not shown in this table (D day is assumed as 2025/3/6).

Phase	Maneuver	Start Time	Duration (day)	Delta V (m/sec)	Fuel Used (kg)
Launch	Launch	D day	n/a	n/a	n/a
GTO to Round orbit	Circularize	D+ 294	291	1,608.96	3.30
Earth Escape	Ascending	D+460	176	1,929.55	3.68
Insertion	Deceleration	D+468	10	120.81	0.22
Circularize	Descending and circularize	D+634	150	481.30	0.87
	Total	D+634	627	4,140.62	8.066

2.1.2. The LIONER system

The LIONER system consists of three segments, the space, ground and launch segment. The space segment is LIONER itself containing six subsystems and five scientific payloads. The ground segment includes the **Deep Space Network (DSN)**, **Mission Control Center (MCC)** and data distribution center. Finally, the JAXA H-IIA launch vehicle is chosen to be the launch segment. Therefor, LIONER is expected to be launched in a piggy-back form.

There are seven subsystems in the LIONER microsatellite including **Structure and Mechanisms Subsystem (SMS)**, **Thermal Control Subsystem (TCS)**, **Attitude Determination and Control Subsystem (ADCS)**, **Propulsion Subsystem (PS)**, **Electrical and Power Subsystem (EPS)**, **Telemetry and Tracking and Command subsystem (TT&C)**, and **Command and Data Handling subsystem (C&DH)**. The five scientific payloads, including LRO receiver, IES(Ion and Electron Sensor), MAG(Magnetometer),SHEPP (Solar High Energy Particle Probe and IES, are installed onboard LIONER. Detailed descriptions of each subsystem and payload are shown in Table 4.

Table 4. Mass budget ,the mass of each component and the total mass of LIONER.

Instrument	Qtn	Unit Weight (g)	Instrument	Qtn	Unit Weight (g)
SMS	1	9,414	Transmitter of S band	1	70
Reaction wheel	4	240	Receiver of occultation NovaTel OEM 719	1	31
IMU	2	70	Antenna of X band	1	17
Gyroscope	2	90	Antenna of S band	2	100
Sun seneor	2	300	Antenna of occultation	1	80
Star tracker	2	245	Fuel	1	10000
LAICA	1	1,650	Tank	1	700
Solar cell	400	2.752	RIT-10 evo thruster	1	1,800
Solar cells, unfold device	2	500	ISIS On Board Computer	1	94
Battery	3	2,790	SHEPP	1	135
Modular power system PDRU	1	182	IES	1	1,040
DC-DC converter	1	30	MAG	2	545
Transmitter of X band	1	270	TCS	1	1000
Receiver of S band	1	200	Harness	1	3,000
TOTAL					43.734 kg (~12.5% margin left)

2.2. Space segment: the LIONER microsatellite

The configuration of the LIONER microsat is shown as Fig. 16. It is noted that the deployable solar array is not shown in this figure. The illustration and animation of the deployment of the LIONER solar panel can be found by <https://goo.gl/DZCcWr>.

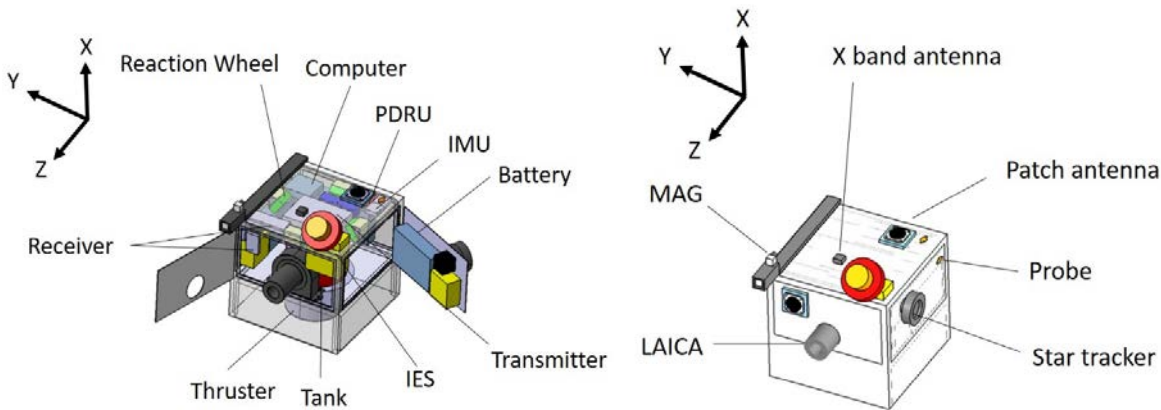


Figure 16. The major components of the LIONER microsatellite

2.2.1. Structure and mechanism subsystem (SMS)

The method and procedure of designing the main structure of LIONER is followed by the description in the thesis written by Ching-Lung Chiang [12], and a computer aided design software CATIA is used to design the structure and simulate the responses under different scenarios. Figure 17 shows the flow chart of the design of SMS. The mechanical parameters such as the total mass, the center of the mass, moment of the inertia can be calculated by CATIA directly. Further modal and stiffness analysis can be performed with Aboqus, and the mechanical design is carefully checked to satisfy the requirements of the launch vehicle and mission operation.

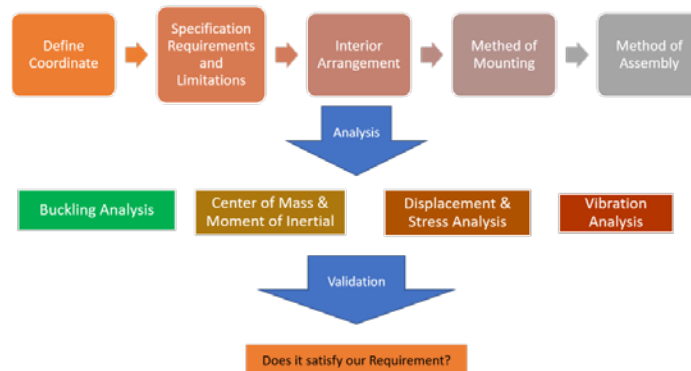


Figure 17. The flow chart for SMS design including specifying the requirements, analyses, and validation.

2.2.1.1. Coordinate Definition

A clear definition of the satellite coordinate is not only one of the most important requirements of designing a satellite system, but also will provide us a good picture for arranging the instruments to perform the best measurements. Figure 18 shows the schematic of the LIONER coordinate system, and Table 5 summarized the local horizontal and vertical coordinates for the LIONER mission.

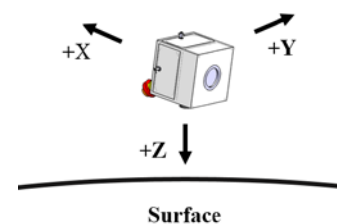


Figure 18. The coordinate system for the LIONER satellite

Table 5 Local horizontal local vertical (LVLH) coordinates for LIONER mission phase.

Position	Earth/Moon orbit		Cis-lunar cruise	
Axis	+X	+Z	+X	+Y
Direction	Ram direction	Nadir direction	Ram direction	Starboard direction
General Requirement	1. Solar panels have to face to sun. 2. Thruster will be put on the wake direction on -X panel. 3. Communication system can't be put at nadir direction toward moon. 4. LAICA has to face to the Earth or the Moon . 5. Two star trackers will be mounted for opposite directions to ensure the navigation capability even one star tracker cannot work when sun is in the field of view of it.			

2.2.1.2. Structural Requirement

During structural design process, LIONER will have to satisfy the requirement of launch environment provided by the H-IIA rocket as summarized in Table 6-9. To fly the satellite out to space, the launch mass of the satellite cannot exceed 50 kg, and the length, width and height has to be within 50 cm, respectively. In order to extend IES out of the structure and place solar panels, the main structure is shrunk to increase available external space.

Table 6. Quasi-Static Acceleration.

Axis direction	Axis orthogonal direction
-6 G / +5 G	±5 G

Table 7. Sine Wave Vibration.

	Axis direction	Axis orthogonal direction
Frequency	5 ~ 100	5 ~ 100
Acceleration	2.5 G	2 G

Table 8. Random Vibration

Frequency Width(Hz)	Acceleration (G ² /Hz)
20 ~ 200	+3 (dB/octave)
200 ~ 2000	0.032 G ² /Hz
Effective value	7.8 (Grms)

Table 9. Rigidity requirement.

Axis direction	Axis orthogonal direction
more than 120 Hz	more than 60 Hz

2.2.1.3. Material selection

The importance of the structure is to withstand high acceleration and violent vibrations, and to protect the satellite from being damaged. During the design process, the design should meet the restriction of launch mass, the specification of launch vehicle and space environment when it's in operation.

The 7075 aluminum alloy is selected as the frame material mixed with zinc, which has great fatigue resistance properties, is the common material in aerospace engineering. The alloy is the mixture of aluminum, zinc, magnesium and copper(Al-Zn-Mg-Cu), Table 10 summarizes the selected parameters of the alloy.

Table 10. Properties of the material 7075 aluminum alloy.

Specific weight	2.80 g/cm ³
Elastic Modulus	7.3
Specific heat (0~100°C)	0.23 cal/g · °C
Linear expansion rate (20~100°C)	23.6
Young Modulus	7.17×10 ¹⁰ N/m ²
Poisson's ratio	0.33

2.2.1.4. Structural analysis

Abaqus is used to analyze the natural frequency of the structure and the response at some specific accelerations, preventing resonance due to the same frequency of vibrating environment and natural frequency of the structure, which is usually the main reason of fatigue destruction. By performing analysis during design process, some parameters or configurations can be modified to prevent above problems.

2.2.1.4.1. Modal analysis

There are 10 modes to be calculated to know under which frequency the structure will be strongly affected. Table 11 shows the first 10 natural frequencies of the LIONER system. Figure 19 shows the final shape of the structure and stress distribution under different modes the areas in red represent that they are highly stressed while those in blue indicate lower-stressed parts.

Table 11. First 10 Natural frequencies.

Mode	Frequency(Hz)	Mode	Frequency(Hz)
1	236.75	6	500.78
2	340.95	7	542.19
3	385.10	8	645.75
4	409.94	9	651.57
5	450.66	10	717.95

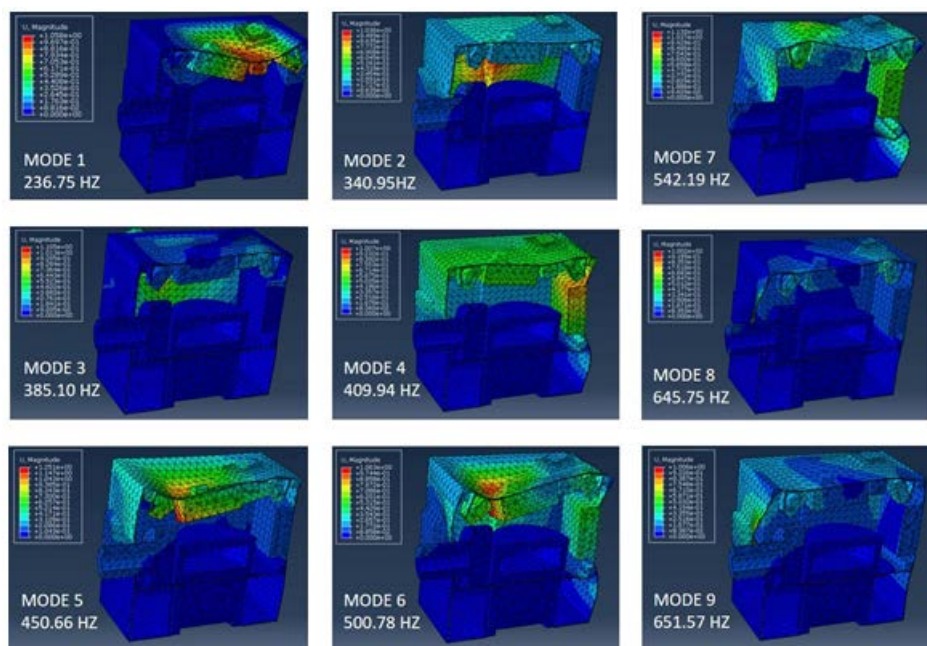


Figure 19. Illustration of modal analysis, from modal analysis of Aboqus, the first mode will occur at 236.75 Hz, larger than contest requirement of 100Hz. Knowing different mode can prevent LIONER from fatigue under these conditions.

2.2.1.4.2. Random vibration analysis

The analysis of random vibration is able to predict the response of a system when it's under continuous oscillation caused by external forces, presenting the response to shocks of the environment from the satellite structure during the transportation.

Figure 20 shows that the situation in which the point is exerted a force by picking a point on the fixed surface and calculating its RF3. Figure 21 with the magnitude falling in the range of the average plus and minus a standard deviation (which contains 68% of samples) can be predicted.

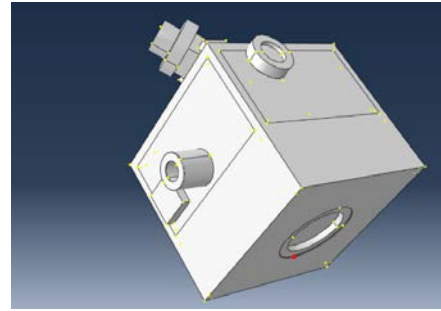


Figure 20. The the reaction forces which a point on the surface are applied when the frequencies of vibration are between 1~2000 Hz. While doing the design, one should avoid perturbation with these frequencies.

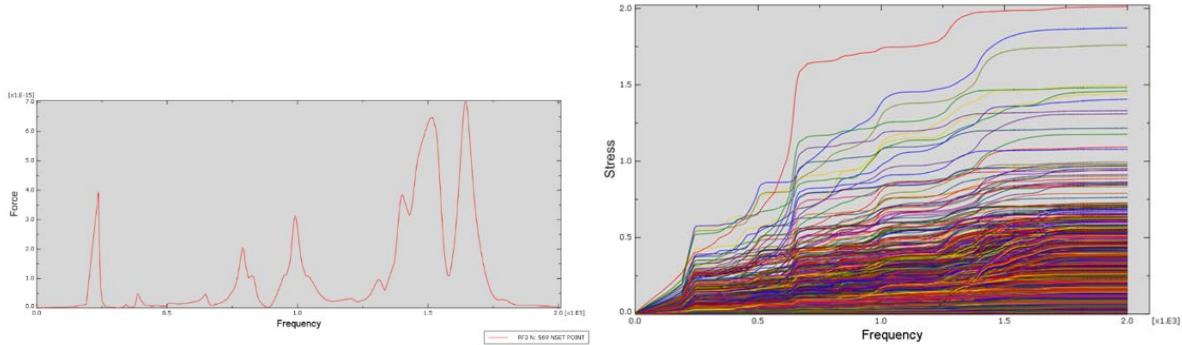


Figure 21. Force-frequency diagram. Figure 22. The variation of stresses with respect to frequencies at every point on the surface. The maximum stree is 2.1 MPa, and the materials won't fail under such a stress.

2.2.1.4.3. Stiffness analysis

Stiffness analysis, one of the structural analysis, is used for the determination of the effects of loads on physical structures and their components. Clamping the ram and wave direction with upward acceleration of 50 m/s^2 , the stress distribution on the structure shows only limited deformation.

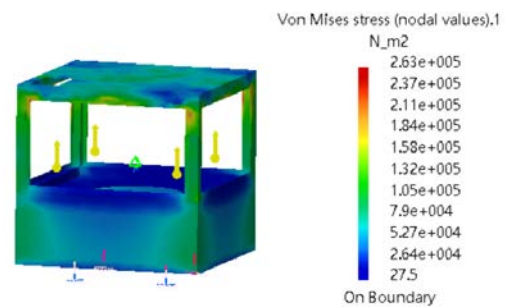


Figure 23. Illustration of acceleration analysis

2.2.1.4.4. Honeycomb structure

Aluminum alloy honeycomb structure are commonly used in aerospace vehicles due to its appropriate properties on energy absorption, heat transfer, electromagnetic shielding and high strength to weight ratio [13].

The performance of honeycomb mainly depends on its relative density, as the relative density raised, so as its stiffness. We define relative density as $\rho = \rho^* / \rho_s$, with ρ^* represents the density of honeycomb and ρ_s is the density of the substance. For honeycomb structure with no specific shape, assuming the length of the hole is l and the thickness the wall of hole is t as

shown in Fig. 24 When $t \ll l$ the material has low relative density, where the relationship can be represented as

$$\frac{\rho^*}{\rho_s} = C \frac{t}{l}, \quad - (2)$$

Where C is the shape parameter. By changing the ratio of t and l the stiffness of the structure can be determined. Using honeycomb panel from Aerospace Industry Development Corporation (AIDC), the thickness of wall, t, is 0.15mm, l is 3 mm, h is 4mm. According to Cellular solids: structure and properties from Lorna J Gibson Micheal F.Ashby [14], ρ^*/ρ_s of an hexagonal structure can be computed from the following equation [15]:

$$\frac{\rho^*}{\rho_s} = \frac{2}{\sqrt{3}} \frac{t}{l} \left(1 - \frac{1}{2\sqrt{3}} \frac{t}{l} \right) \quad - (3)$$

In our case the relative density $\frac{\rho^*}{\rho_s}$ is 0.057, take the area of $240 \times 360 \text{mm}^2$ and the mass of Aluminum with thickness of 2 mm $mass_o$ and honeycomb structure of 5 mm thickness $mass_h$ will be

$$mass_o = 2.8 \text{ g/cm}^3 \times (0.2 \text{ cm} \times 24 \text{ cm} \times 36 \text{ cm}) = 483.84 \text{ g}$$

$$mass_h = 2.8 \text{ g/cm}^3 \times [(0.1 \text{ cm} \times 24 \text{ cm} \times 36 \text{ cm}) + 0.057 \times (0.4 \text{ cm} \times 24 \text{ cm} \times 36 \text{ cm})] = 297.08 \text{ g}$$

In planform area, the mass can be reduced by 38% which means 2,500g.

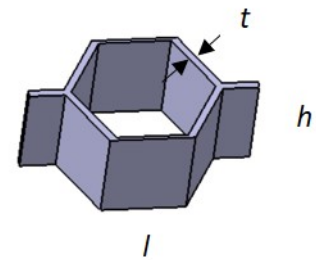


Figure 24. The cell of honeycomb.

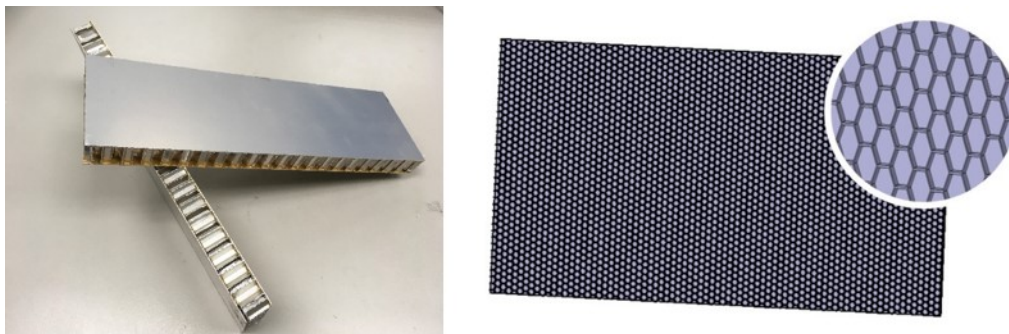


Figure 25. (Left) Honeycomb sample with military specifications. (Right) The profile of panel of z axis and the size is 5 mm×(with core of 4 mm, 1 mm of upper and lower) $240 \times 360 \text{mm}^2$.

2.2.2. Thermal control subsystem (TCS)

Each instrument on LIONER has its range of operating temperature. If LIONER is exposed under a temperature out of the range of storage temperature, an instrument may be permanently damaged, leading to a fail mission. Thus, the thermal analysis makes a vital part. The operating temperatures for each component are summarized in Table 12 .

Table 12. Shows the operation temperature and heat generation of each instruments.

System	Instrument	Operation Temperature(°C)	Heat dissipation (W)	System	Instrument	Operation Temperature(°C)	Heat dissipation (W)
ADCS	Reaction wheel	-40 ~ 80 (assume)	4	C&DH	Computer (ISIS)	-25 ~ 65	0.55
	IMU	-40 ~ 85	2.2	EPS	Battery	-10 ~ 35	0
	Gyroscope	-40 ~ 80 (assume)	2.4		Solar panel	-150 ~ 100	0
	Sun sensor	-40 ~ 80 (assume)	2		PDRU	-35 ~ 85	0

TT&C	Star tracker	-30 ~ 60	2	Payload	LAICA	-20 ~ 40	10
	Transmitter (X band)	-20 ~ 60	12		IES	-40 ~ 80 (assume)	1.85
	Receiver (S band)	-30 ~ 75	1.5		Solar probe	0 ~ 70	0.8
	Transmitter (S band)	-40 ~ 80	2.5		Receiver (occultation)	-40 ~ 85	1.5
	Antenna (X band)	-40 ~ 85	0		Magnetometer	-160 ~ 120	0.84
	Antenna (S band)	-20 ~ 50	0	PS	Thruster	-85 ~ 140	219.28 (assume)
Structure	Frame	N/A	0		Tank	20 ~ 50	0

In order to make good assumption of thruster dissipation, we first calculate the kinematic energy of ejecting particales by following equation, where V_{beam} and m_{ion} are velocity and atomic mass of leaving particales respectively respectively. Therefore, the kinematic energy per second is 215.72 J/s , and the dissipation is electricy power minus kinematic energy per second, i.e. 219.276W when the thruster is operated.

$$V_{beam} = \eta_m \sqrt{\frac{2Ue}{m_{ion}}} \quad - (4)$$

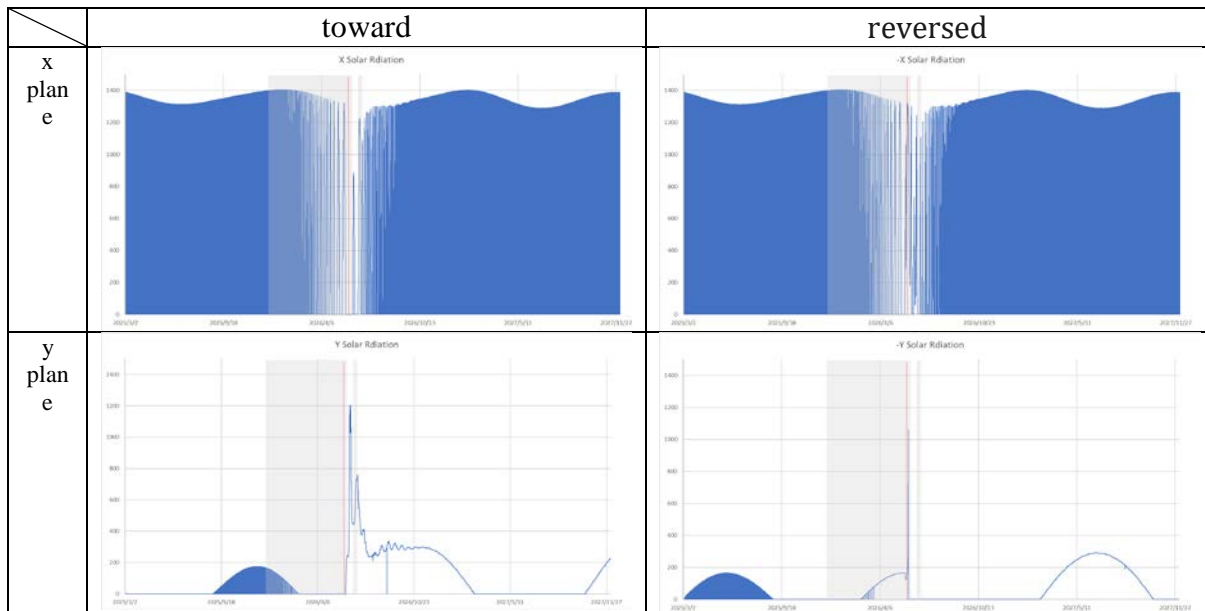
The only thing that TCS needs to do is finding the hottest and coldest condition from beginning of life (BOL) to end of life (EOL). After that, trying to conquer two of them by using sutible coating on surface and power for heater respectively. To figure out hottest and coldest period, solar radiation, planet's infrared, exposure area, coating and heat dissipation are all our consideration.

Thermal environment

Solar radiation is the essential radioation from the space, so the hottest condition could encounter more radiation than other days. Fig.26 shows the different plane of actual solar flux i.e.

$$solar\ flux \times solar\ intensity \times \cos\theta$$

from BOL to one year after arriving Moon parking orbit, where θ is definid by Fig.27. Obviously, y-plane will encounter lowest solar flux, so the best design is to reject heat dissipation toward y-plane or reversed y-plane properly. At the same time, applying high emissivity/absorbability ratio to $\pm y$ plane's surfaces and applying silver or MLI at others surfaces to lower the sensitivity to Sun is needed.



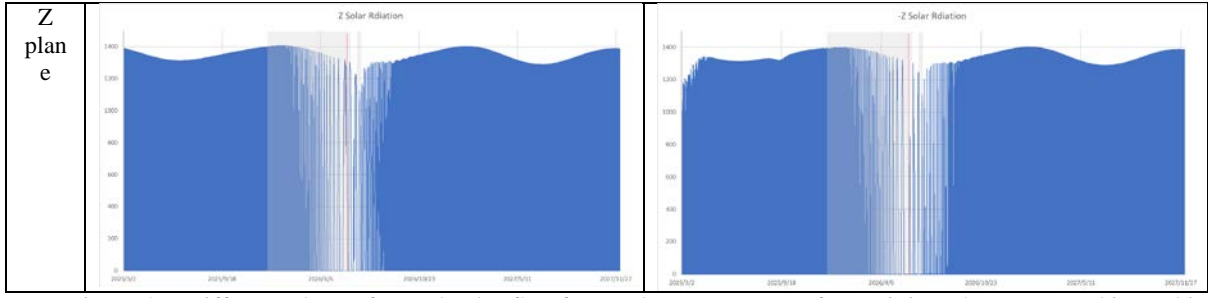


Figure 26. Different plane of actual solar flux from BOL to one year after arriving the Moon parking orbit. Gray area means that ion engine is operated most frequently, and orange line means the time change coordinate from Earth to Moon.

Especially, the surface of LIONER will also encounter Earth or Moon infrared, albedo, and the magnitude and direction of net flux will calculate by Eq.5 Eq.6 Eq.7 [16],

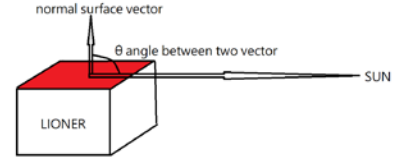


Figure 27 . Illustration of angle θ between normal surface vector and sun vector.

$$Q_{planet \text{ to } n \text{ direction of LONER}} = \frac{A_n \sigma (T_{planet}^4 - T_{LIONER}^4)}{\frac{1}{F_{L_n \text{ to } pl}} + \frac{1 - \alpha_n}{\epsilon_n}} \quad - (5)$$

$$F_{LIONER_{+z} \text{ to } planet} = \left(\frac{R_{planet}}{H_{planet}} \right)^2 \quad - (6)$$

$$F_{LIONER_{\pm x,y} \text{ to } planet} = \frac{1}{\pi} \left[\tan^{-1} \left(\frac{R_{planet}}{\sqrt{R_{planet}^2 + H_{planet}^2}} \right) - \frac{R_{planet} \sqrt{R_{planet}^2 + H_{planet}^2}}{H_{planet}^2} \right] \quad - (7)$$

wherer σ is Stefan–Boltzmann constant, R_{planet} is the radius of planet, H_{planet} is distance from LIONER to heart of planet, A_n is the n direction of area of LIONER, α_n and ϵ_n are absorptivity and emissivity of n direction, F is view factor and T_{planet} will follow by Fig.28. Albedo value of Earth and Moon are 0.367 and 0.136 respectively.

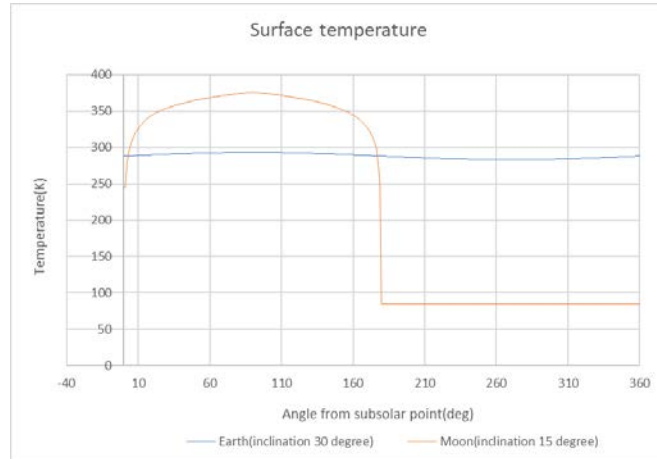


Figure 28. Surface temperature of Moon and Earth

Governing equation

To simplify the analysis, we first made the following hypotheses:

1. All instruments consist of 7075 aluminum alloy which is the same as the structure of LIONER.
2. Their conductivity and specific heat are constants, $130(\text{W}/\text{m} \cdot \text{k})$ and $960 (\text{J}/\text{kg} \cdot \text{K})$, respectively.

3. The thermal coating will be applied in each surfaces of instruments to increase conductivity, so there's no conduction heat resistance within the structure and to reduce temperature gradient for each instruments using filler.
4. If the internal temperature difference is small, radiation between instruments can be neglected. Therefore, the complicated view factors don't have to be calculated.

After considering space environment, LIONER will calculate more accuracy temperature at any time by the following equation. First, deriving the equation of energy conservation for each instrument Eq.8.

$$\sum_{i=1}^n \dot{Q}_{i\ net} - \sum_{i=1}^n \dot{W}_{i\ out} + \sum_{i=1}^n \dot{E}_{i\ g} = \sum_{i=1}^n \frac{\partial \dot{E}_i}{\partial t} \quad - (8)$$

$$\sum_{i=1}^n \dot{Q}_{i\ net} - \sum_{i=1}^n \dot{W}_{i\ out} + \sum_{i=1}^n \dot{E}_{i\ g} = \sum_{i=1}^n \frac{d\dot{E}_i}{dt} \quad - (9)$$

Since heat conduction at inner LIONER is faster than outer surface which radiates heat rate to the space. LIONER will be considered as a lump system, ie, instruments are isothermal objects. Therefore, Eq.8 becomes to Eq.9. There is a difficulty that if LIONER have hundreds of component, and hundreds of equation of energy conservation could be solved case by case. Therefore, to monitor easily, LIONER will adopt conductor and heatpipe that will be installed in honeycomb panels to simplify analysis. The conductor, Annealed Pyrolytic Graphite (APG), with conductivity 1,700 W/m-K at room temperature can transfer heat efficiently and make the LIONER more closely to a lump system. The similar temperature range of each instrument will be fixed to panels, and it will be adjacent to same line, which is made of APG and heat pipe. Table 13 shows 3 main line, and other components will be calculated independently. In that case, these instruments can be considered as having the same temperature. So, we can reduce solving each components' energy equations to 7 categorizes. Fig.29 shows that A, B and C line couple to geometry.

Table 13. shows 3 different heat pipe to simplify TCS

A line (-40~80°C)	B line (-20~60°C)	C line (-10~35°C)	Others
Reaction wheel IMU Gyroscope Sun sensor Transmitter S Receiver(ocutation) Antenna of X band IES PDRU	Receiver S Transmitter X Antenna of S band Star tracker Computer Solar Extreme Ultraviolet Probe	Battery LAICA	Thruster Solar array Tank MAG

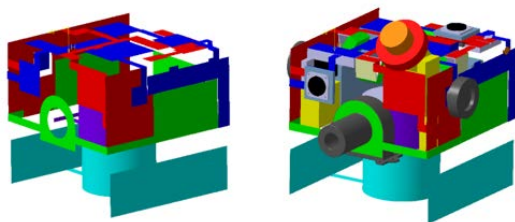


Figure 29. Isothermal line made by APG and heat pipe and red is A line, blue is B line, and green is C line

The calculation will be started when knowing all parameter such as surfaces, radiation, mass and conductivity. The extreme cases that will be test firstly in Fig.30 could probably hot case or cold case, which is predicted by beta angle Fig.31. Next, temperature at that period of time can be calculated in Matlab. If the maximum temperature in Matlab is larger than operating temperature, first action is changing coating parameter. If that can't afford hot case anymore, second trying is changing $\pm y$ radiation's surface area which could fulfill by enlarging

APG area. However, hot and cold case should rediscover when changing radiation's surface. The calculate scheme shows in Figure 32.

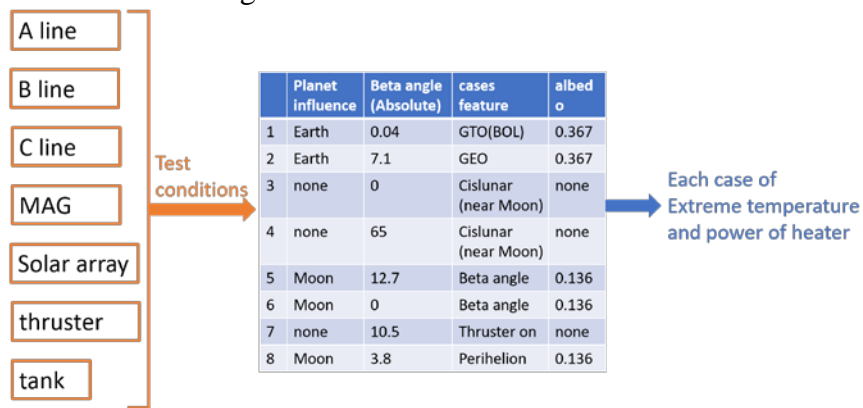


Figure 30. the process of finding extreme temperature (Extreme cases of environment is predicted by beta angle & dissipation.)

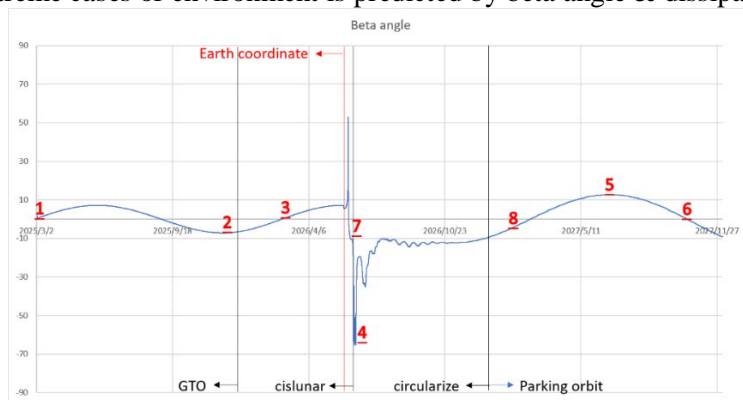


Figure 31. the time of extreme cases

The features of TCS are following items and showed in Fig.33

1. Insulated all of propulsion components from structure for tank.
2. Outer surface of X,Z panel will covered with beta cloth MLI
3. The thermal coating will be applied in each surfaces of instruments to increase conductivity, so that there's no conduction heat resistance within the structure and reducing temperature gradient for each instrument by using filler.
4. Outer components of LIONER will be covered with 10 mil white silicone paint around exposed surface to reduce radiation.
5. Inside surface painted Kapton Laminate to separate each line as possible.
6. Insulated between MAG and hinge.
7. Using APG and heat pipe as the conductor to transfer heat and coupling similar temperature range components.
8. Using deployable radiators to control the direction of heat flow. Rejecting heat from thruster to space in y directon. In contrast, absorbing heat from x plane when radiator is colsed.

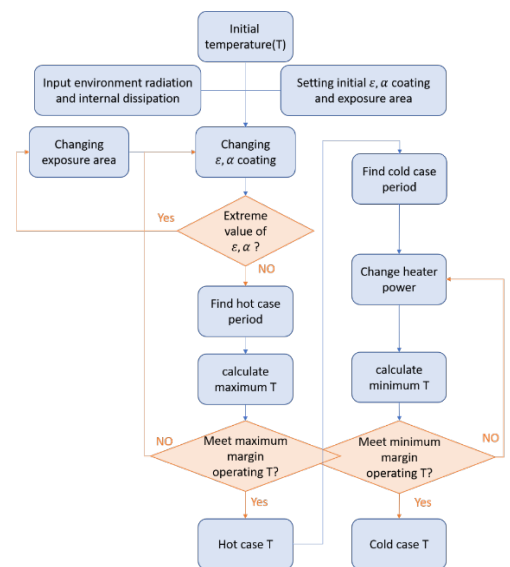


Figure 32. The scheme of TCS

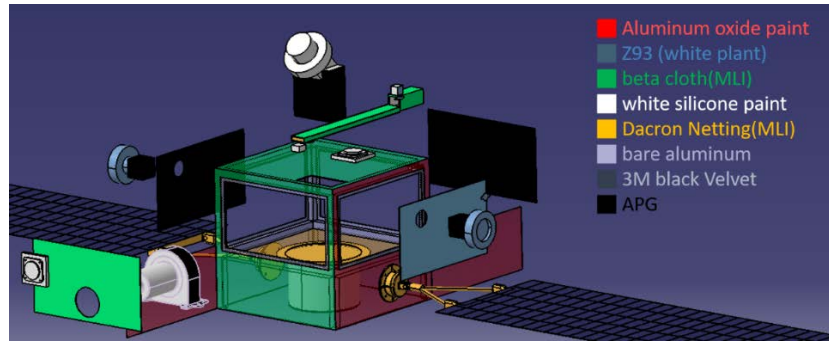


Figure 33.the geometry of LIONER thermal components.

It is a most important part of thruster. After calculation of hot case of thruster, the radiation area is $0.35m^2$, we have no choice but to adopt deployable radiator shown in Fig. 34. In hot case, the radiator will unfasten to reject large heat, and pick it up to absorb solar radiation to maintain turn-off period.

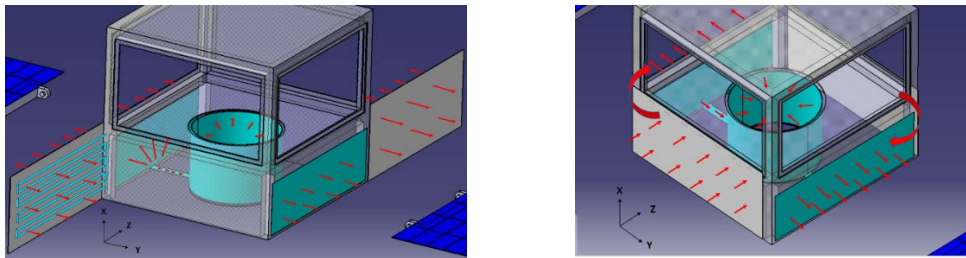


Figure 34. The emphasis of thruster section heat flow(read arrow) of hot case and cold case.

The final result of TCS are summarized in Table 14, Fig.35 and the hot cases and cold case of individual components temperature curve are placed in Appendix I.

Table.14 The final coating parameter choosing in each surface [17].

	BOL	EOL	BOL	EOL	apply location
	ϵ (emissivity)		α (absorbility)		
10 mil white silicone paint	0.88	0.88	0.22	0.46	$\pm x, \pm z$ side of outer instruments
Z93 (white plant)	0.92	0.92	0.18	0.55	$\pm y$ plane, $\pm y$ side of outer instruments
Aluminum oxide paint	0.92	0.92	0.09	0.09	$\pm y$ plane, radiator connet to thruster
FSS-99(Metallic)	0.02	0.02	0.03	0.03	-y plane area conneted to tank
3M black Velvet	0.91	0.84	0.97	0.97	Back side of solar array
beta cloth(MLI)	0.86	0.86	0.4	0.4	$\pm x, \pm z$ plane

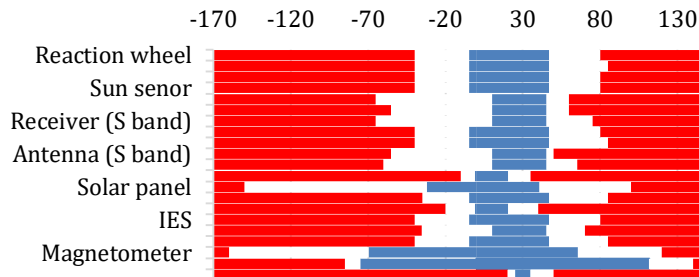


Figure 35. Operation range of tempratute in each case, and blue line shows precict tepereture and red line shows tempratute limit, respectively.

2.2.3. Attitude determination and control subsystem (ADCS)

Figure 36 shows the architecture of the ADCS for LIONER. The field of view (FOV) and target of view of the LAICA is 5.71 degree and 2.86 degrees, respectively. Pointing accuracy which is about one-tenth of target of view (around 0.29 degree) makes more than 99.7% target

of view falling into FOV. Zero momentum control method has an accuracy of 0.1 degree which meet the requirement. Sun sensor, star tracker, gyroscope, and IMU are used to detect attitude of satellite. Sensors with accuracy better than 0.1 degree meet the requirement of error calculation to control the satellite. Disturbance of the lunar gravity is affected by the gravity of Moon ($\mu = 4.903 \times 10^{12} m^3/s^2$), orbit radius of LIONER ($R=3,737km$), and moment of inertia about x and z axis (I_x, I_z). According to equation 10 , disturbance on lunar orbit is around 10^{-7} , which means the requirement on controlling the altitude isn't large.

$$T_g = \frac{3\mu}{2R^3} |I_z - I_x| \sin(2\theta) \quad - (10)$$

Since there is no GPS system to provide navigation, IMU is used to calculate position to a relative frame. However, GPS receiver is needed when satellite is in Earth Orbit phase to check if all instruments can work normally.

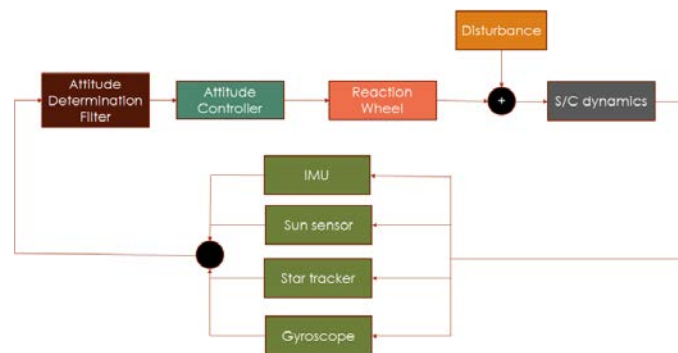


Figure 36. The architecture of ADCS in the LIONER satellite.

Table 15. Properties of sensors.



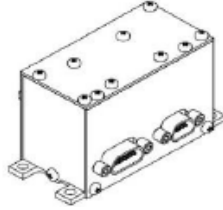


	star tracker	sun sensor	Gyroscope
			
Exclusive angle	> 35 degrees	-32 ~ 32 degrees	-250 ~ 250 deg/s
accuracy	< 7 arcsec (3σ)	0.1 degrees	up to 0.005 deg/s
Power	< 1 W	< 1 W	1.2 W
Mass	245 g	300 g	90 g
Dimensions	50×50×113 mm	96×94×53 mm	34×38×66 mm
Unit	2	2	2

Table 16. Actuator and Navigation instrument.

Reaction wheel		IMU	
			
Mass	0.24 kg	Mass	0.07 kg
Volume	58×58×25 mm	Volume	47×44×14.2 mm
Momentum	0.05 Nms	Angular rate control performance	0.153 °/s (1σ)
Power consumption	<0.5 W (0.5 momentum) <1.0 W (full momentum)	Gyroscope operation range	Up to 500 deg/sec in all axes
		Accelerometer operation range	Up to 16 G in all axes
		Magnetometer operation range	Up to 16 gauss in all axes
		Power consumption	< 1.1 W
Unit	4	Unit	2

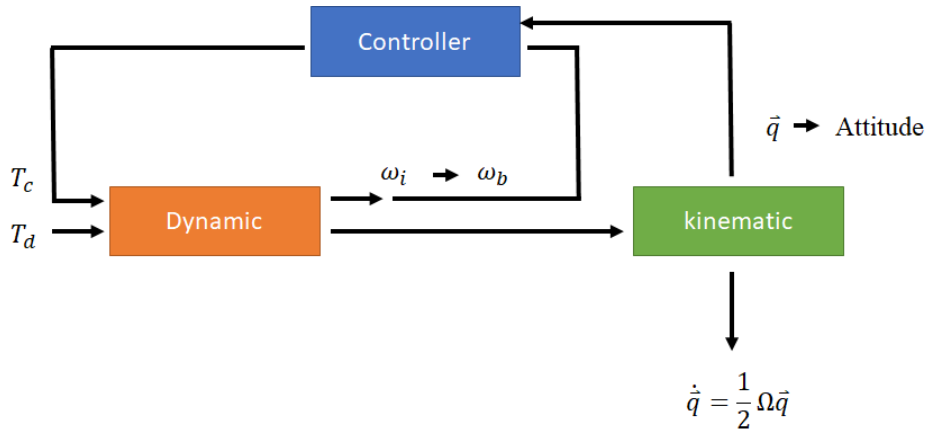


Figure 37. Flowchart of dynamics and kinematics simulation

Figure 37 shows the flowchart of dynamics and kinematic simulation. Dynamics of the LIONER can be derived from equation (11). No disturbance is included.

$$I_S \vec{\omega}_i = \vec{\omega}_i \times (I_S \vec{\omega}_i + \vec{h}_\omega) - \vec{h}_\omega \quad - (11),$$

where $I_S = \begin{bmatrix} I_x & 0 & 0 \\ 0 & I_y & 0 \\ 0 & 0 & I_z \end{bmatrix}$ is moment of inertia, and $\vec{\omega}_i = \begin{bmatrix} \omega_{x,i} \\ \omega_{y,i} \\ \omega_{z,i} \end{bmatrix}$ is body angular rate in

ECI frame. By the following equation, attitude of LIONER in ECI frame can be derived.

$$\frac{d}{dt}\vec{q} = \frac{1}{2} \begin{bmatrix} 0 & \omega_{z,i} & -\omega_{y,i} & \omega_{x,i} \\ -\omega_{z,i} & 0 & \omega_{x,i} & \omega_{y,i} \\ \omega_{y,i} & -\omega_{x,i} & 0 & \omega_{z,i} \\ -\omega_{x,i} & -\omega_{y,i} & -\omega_{z,i} & 0 \end{bmatrix} \vec{q} \quad - (12),$$

where \vec{q} is quaternion vector. Transforming quaternion to Euler angles (under ECI frame) can acquired the attitude of LIONER. For the purpose of analysing stability of LIONER, frame of attitude is transformed from ECI frame to Body frame by equation 13. Detailed can be find in Ref [18].

$$\begin{bmatrix} \varphi_b \\ \theta_b \\ \psi_b \end{bmatrix} = \begin{bmatrix} 1 - 2(q_2^2 + q_3^2) & 2(q_1q_2 + q_3q_4) & 2(q_1q_3 - q_2q_4) \\ 2(q_1q_2 - q_3q_4) & 1 - 2(q_1^2 + q_3^2) & 2(q_2q_3 + q_1q_4) \\ 2(q_1q_3 + q_2q_4) & 2(q_2q_3 - q_1q_4) & 1 - 2(q_1^2 + q_2^2) \end{bmatrix} \begin{bmatrix} \varphi_i \\ \theta_i \\ \psi_i \end{bmatrix} \quad - (13)$$

φ, θ, ψ are angle of three axis. Figure 38 shows the results on lunar orbit, that the selected reaction wheel meet the requirement. Angular rate in ECI frame is $\omega = [0.0000997, 0, 0.000282]$ rad/s.

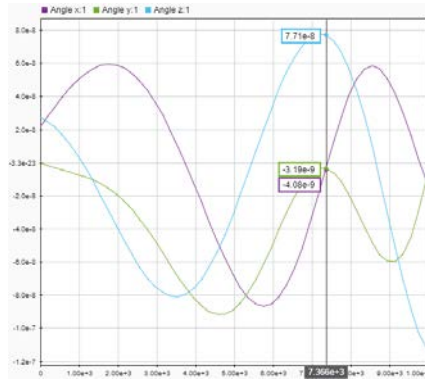


Figure 38 . The attitude of LIONER with initial condition ($q = [0.7071, 0, 0.7071, 0]$), unit of x-axis is second, and the unit of y-axis is rad/sec.

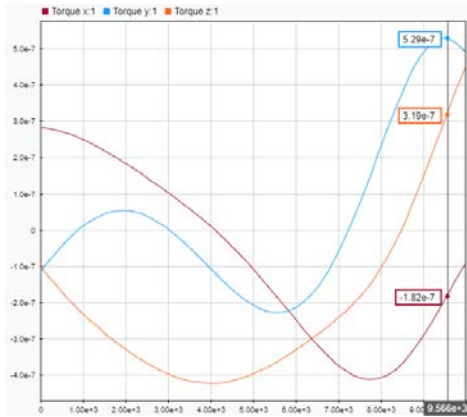


Figure 39. Torque output from the reaction wheel in three axis, and the unit of x-axis is second, unit of y-axis is N·m.

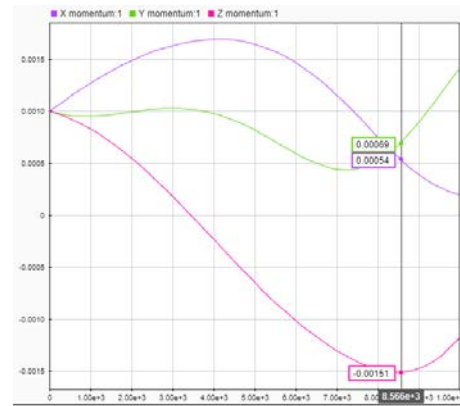


Figure 40. Momentum output from the reaction wheel in three axis, unit of x-axis is second, and the unit of y-axis is N·m·s.

The propulsion system of LIONER includes a thruster and the feul tank component. To save fuel for transferring to the Moon, LIONER adopts an ion propulsion method and uses ion thruster as the engine. RIT 10 EVO is selected as the thruster due to relatively high thrust, low dead mass and high specific impulse after careful survey. This engine has been operated in space with high reliability. The carbon composite tank will be a cylinder with the radius of 10

cm and height of 10.6 cm. The selected specifications of RIT 10 EVO thruster are listed in Table 17.

Table 17. Properties of thruster

I_{sp}	3000 s
Maximum thrust	15 mN
Diameter	186 mm
Height	134 mm
Mass	1.8 kg
Power consumption	435 W



Figure 41. RIT 10 EVO Thruster

2.2.4. Electrical power subsystem (EPS)

The EPS shall supply electricity to each subsystems and payloads during the mission. The EPS is composed by the solar cells, batteries, and Power Distribution and Regulation Unit (PDRU). The PDRU allocates power to each subsystems and payloads based on the commands from C&DH. The PDRU ensures each subsystems and payloads having nominal current and voltage, and can regulate 3.3V, $\pm 5V$, 8V, $\pm 12V$, and 18V. To satisfy the requirements, Modular power system produced by GOM space is installed to be the LIONER's PDRU.

The huge energy consumption of the thruster of LIONER requires 900 volt. To provide high voltage to the thruster, MIL-COTS DCM DC-DC Converter Module produced by Victor will be installed to boost the input voltage to at least 900V. Our largest power consumption is 499.04W, and the size and characteristic of DC-DC converter are usually decided by the power of the system. So we choose DCM 4623 ChiP which can provide 500W as a reference to design the EPS system. Figure 42 shows the functional block diagram of the EPS.

Ten solar cells will be connected in series as one group, and there are 20 groups connected in parallel to compose one of two solar panels. This will provide 24.11V for charging batteries. The detail properties of the battery and solar cell are listed in Table 18.



Figure 42. Functional block diagram of the EPS subsystem

Table 18. Properties of battery and solar cell.

Battery		Solar cell	
Lithium ion cell for satellite applications LSE100		C4MJ Solar Cells	
Manufacturer	GS Yuasa	Manufacturer	SPECTROLAB
Nominal voltage (V)	3.7	Solar Flux Density (W/m ²)	1367
End of charge voltage (V)	3.7	Solar Cell Efficiency (%)	30
End of discharge voltage (V)	3.65	Voltage at max. Power (V)	2.411
Nominal capacity (Ahr)	110	Current at max. Power (A)	0.504
Dimension (mm ³)	130 × 50 × 208	Average Open Circuit (V)	2.7
Weight (kg)	2.79	Average Short Circuit (A)	0.5202
Quantity	3	Dimension (mm ²)	40 × 80
		Quantity	400

2.2.4.1. Solar Panel and Battery

LIONER will be installed two solar panels. There are several sources to influence the efficiency of solar cell. Beside the angle of the solar panel and the sun light, the orbit of the satellite also need to be concerned. There are three situations out of eclipse, in the Penumbra, and in the eclipse. The power generation can be known by the equation 14.

$$P_{generation} = n \times A \times \eta_{SC} \times SF \times \cos \beta \times e \quad - (14)$$

Where $P_{generation}$ is the power generated by the solar cells with the unit of W, n is the quantity of the solar cells, A is the cell area for each solar cell with the unit of m^2 , η_{SC} is Nominal Solar Cell Efficiency, SF is Solar Flux Density with the unit of W/m^2 , β is the angle of normal vector of the solar panel and the sun light, and e equals to 1, 0.5 and 0 for out of range of eclipse, in the range of penumbra, and in the range of eclipse, respectively.

LIONER will change its attitude to face sun light when in Earth Escaping, GTO to Round orbit, Cruise, Insertion, Circularize phase to ensure LIONER can maintain enough power for huge consumption of batteries due to ion thruster. When LIONER is in Earth Orbit and Lunar Orbit phase, the power generation is enough, so LIONER doesn't have to face to sunlight all the time to generate power. Moreover, when we reach the Lunar orbit phase, since we don't want to change the attitude for EPS, so the direction of the LRO should be in consideration, so we won't change our attitude for EPS.

The equation of the EPS can be represented by equation 15.

$$C_{remaining} = C_{battery} + \frac{P_{generation}}{V_c} \times t - \frac{P_{consumption}}{V_d} \times t \quad - (15)$$

where $C_{remaining}$ is capacity of remaining batteries with the unit of Ahr, $C_{battery}$ is capacity of batteries with the unit of Ahr, V_c is the charge voltage of batteries with the unit of volt, $P_{consumption}$ is the energy consumption of the LIONER with the unit of W, and V_d represents the discharge voltage of batteries with the unit of volt. The Figure 43 shows the power consumption and power generation in each phase, therefore the LIONER will be installed 400 solar cells and 3 batteries based on the calculation from Eq. 15.

2.2.4.2. Power Budget in Each Mode

LIONER will be turned on after Launch mode and entering Booting mode. C&DH, TCS and TT&C will be turned on in Booting mode, ADCS without the ion thruster will be turned on in Detumbling mode as well, and payloads will be turned on in Cislunar mode and Lunar Science mode. When LIONER is switched to Propulsion mode, payloads will be turned off and the ion thruster will be turned on. The details are listed in Table 19.

Since there are seven phases in Cislunar mode and Lunar Science mode including Earth Orbit, GTO to Round Orbit, Earth Escaping, Cruise, Insertion, Circularize and Lunar Orbit phase, different requirements of instruments in each phase arise. In Propulsion mode, the ion thruster is turned on while payloads are off. The detailed power budget of LIONER is listed in Table 20.

When LIONER is in an emergency, Safe mode will be started to keep the satellite functional. The non-necessary instruments are forced to shut down while only EPS, ADCS, TT&C, TCS and C&DH remain operating. The power budget of Safe mode is listed in Table 21.

Table 19. Power budget in Launch, Booting, Detumbling, Propulsion mode.

Subsystem	Instrument	Consumption (W)	Launch mode	Booting mode	Detumbling mode	Propulsion mode
ADCS	Reaction wheel	4	off	off	on	on
	IMU	2.2	off	off	on	on
	Gyroscope	2.4	off	off	on	on
	Sun sensor	2	off	off	on	on

	Star tracker	2	off	off	on	on
	RIT-10 evo	435	off	off	off	off
TT&C	Transmitter (X band)	14.2	off	on	on	on
	Receiver (S band)	1.5	off	on	on	on
	Transmitter (S band)	2.5	off	on	on	on
C&DH	ISIS	0.55	off	on	on	on
PAYLOAD	LAICA	10	off	off	off	off
	IES	1.85	off	off	off	off
	MAG	0.84	off	off	off	off
	Solar probe	0.8	off	off	off	off
	Receiver (occultation)	1.5	off	off	off	off
TCS			0	16.44	3.84	3.84
TOTAL		481.34	0	35.19	35.19	407.19

Table 20. Power budget in seven phases.

Subsystem	Instrument	Consumption (W)	Cislunar mode						Lunar science mode
			Earth orbit	GTO to round orbit	Earth escaping	Cruise	Insertion	Circularize	Lunar Orbit
ADCS	Reaction wheel	4	on	on	on	on	on	on	on
	IMU	2.2	on	on	on	on	on	on	on
	Gyroscope	2.4	on	on	on	on	on	on	on
	Sun sensor	2	on	on	on	on	on	on	on
	Star tracker	2	on	on	on	on	on	on	on
	RIT-10 evo	435	off	on	on	off	on	on	off
TT&C	Transmitter (X band)	14.2	on	on	on	on	on	on	on
	Receiver (S band)	1.5	on	on	on	on	on	on	on
	Transmitter (S band)	2.5	on	on	on	on	on	on	on
C&DH	ISIS	0.55	on	on	on	on	on	on	on
PAYLOAD	LAICA	10	off	on	off	on	off	on	on
	IES	1.85	off	off	on	on	on	on	on
	MAG	0.84	on	on	on	on	on	on	on
	Solar probe	0.8	off	off	off	off	off	off	on
	Receiver (occultation)	1.5	off	off	off	off	off	off	on
TCS			3	0	30	20	0	0	0
TOTAL		481.34	35.19	477.19	499.04	64.04	469.04	479.04	46.34

Table 21. Power budget in safe mode.

Subsystem	Instrument	Consumption (W)	safe mode						
			Earth orbit	GTO to round orbit	Earth escaping	Cruise	Insertion	Circularize	Lunar Orbit
ADCS	Reaction wheel	4	on	on	on	on	on	on	on
	IMU	2.2	on	on	on	on	on	on	on
	Gyroscope	2.4	on	on	on	on	on	on	on
	Sun sensor	2	on	on	on	on	on	on	on
	Star tracker	2	on	on	on	on	on	on	on
	RIT-10 evo	435	off	off	off	off	off	off	off
TT&C	Transmitter (X band)	14.2	on	on	on	on	on	on	on
	Receiver (S band)	1.5	on	on	on	on	on	on	on
	Transmitter (S band)	2.5	on	on	on	on	on	on	on
C&DH	ISIS	0.55	on	on	on	on	on	on	on
PAYLOAD	LAICA	10	off	off	off	off	off	off	off
	IES	1.85	off	off	off	off	off	off	off
	MAG	0.84	off	off	off	off	off	off	off
	Solar probe	0.8	off	off	off	off	off	off	off
	Receiver (occultation)	1.5	off	off	off	off	off	off	off
TCS			3.84	10.84	32.69	32.69	2.69	12.69	14.99
TOTAL		481.34	35.19	42.19	64.04	64.04	34.04	44.04	46.34

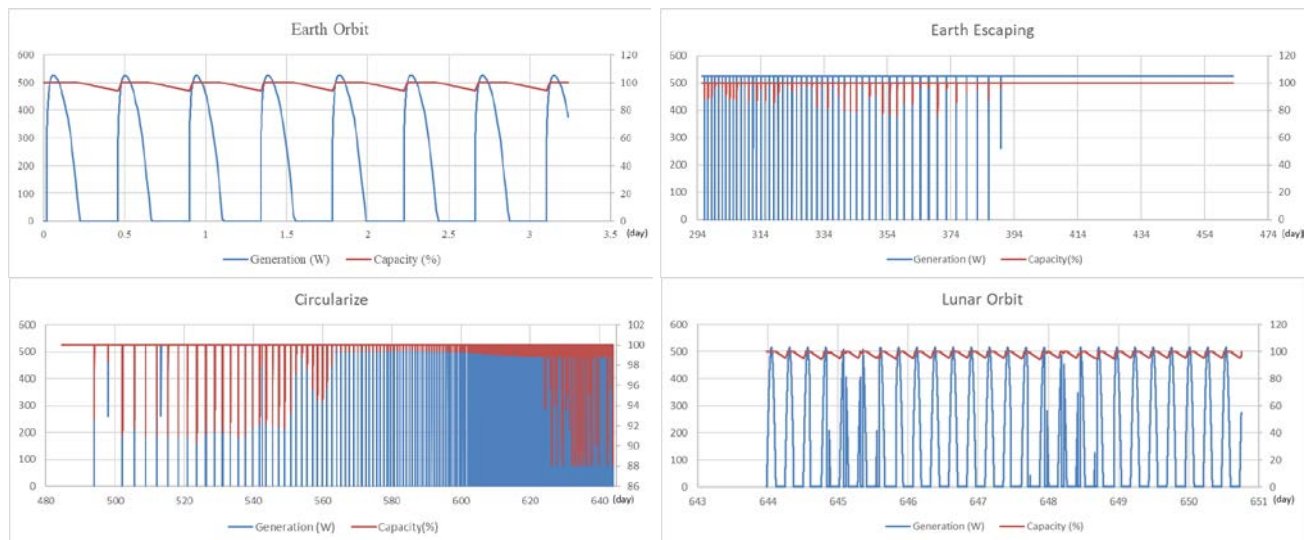


Figure 43. Solar panels generation and battery capacity

2.2.5. Command and data handling subsystem (C&DH)

The command and data handling subsystem is the core of the whole satellite. It has the functions as below:

- Sending command to each subsystem
 - Includes telling EPS how much power it should supply to other subsystems, commanding remaining subsystems and the payload such as IES, LAICA, and the receiver that is used to perform the radio occultation.
- Collecting the data received from payloads and the position information of the satellite
 - The C&DH will collect data from payloads and ADCS into its buffer then pack these data into formatted packets
 - Store the data packets into SD cards.
- Earth communication
 - Carrying out the command from Earth and preparing the data for transmission to Earth.
- Subsystem and payload monitoring
 - The C&DH will continuously monitor the health of each subsystem and payload, and alert anomaly as well as take contingent actions if necessary.

The C&DH subsystem includes the following components:

On board data handling unit: the main C&DH board equips an 400MHz 32-bit ARM9 processor, two redundant Real Time Clocks (RTC), on-board temperature sensor, External on-board watchdog and power-controller.

On board flight software: it includes hardware abstraction layer software which supports I2C interface, I2C is used for attaching lower-speed peripheral ICs to processors and microcontrollers in short-distance and intra-board communication.

Data storage: the on-board computer provides the capacity of two 16GB high reliability SD cards, which stores the science data collected from payloads and the status of the health (SOH) records including temperatures, voltages and currents collected from internal sensors. These data will be stored in the SD cards until they transmitted to the Earth, and then be overwritten by new science and SOH data. Figure 44 shows the functional block diagram of C&DH.

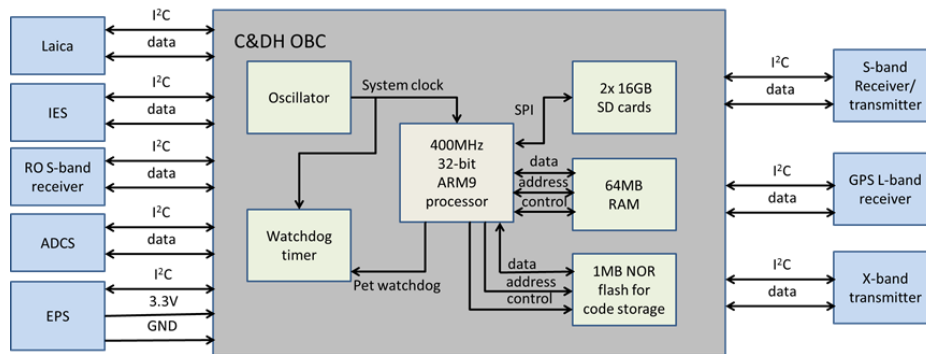


Figure 44. C&DH functional block diagram.

2.2.6. Telemetry, Tracking and Command subsystem (TT&C)

LIONER communicates with the ground station through its TT&C subsystem, it will always stay ready for receiving the command from the ground station, and transmit data including SOH and scientific data to the 70-m antenna of the Deep Space Network (DSN) ground station through X-band and S-band. The satellite uses two downlink band for different purposes. The bandwidth of the S-band is relative small and used to download the SOH data and upload the real-time and time-taged command for the mission operation, and X-band is broader for communication and is able to send large size of scientific data in a shorter time. The satellite receives the operation commands from DSN's 70-m S-band transmitter, whose frequency band is 2110–2118 MHz, enabling the data handling system to distinguish it from LRO's signal frequency (2271.2MHz).

The link budget of the S-band uplink and downlink and X-band downlink between the LIONER microsat at the lunar orbit and DSN 70-m antenna ground station are shown in table 22 and 23. This link budget shows the worst case which is the farthest distance that LIONER can communicate with Earth (~380,000km). Under this circumstance, the path loss of signal is the critical issue to be resolved. It is the major lost compared to all the other facts. In order to send data back successfully to Earth, there are several modification on the previous link budget: first is the transmitting power, higher power output for downlink X-band is needed, while downlink S-band remains the same; second, the decrease of data rate have also been applied to meet the requirement. To ensure that the data rate is enough, the estimation of data size collected by LIONER and the transmission capacity between LIONER and Earth per day is summarized in Table 22.

Table 22 . Estimation of data size per day

IES 1/128sec	1,152 bytes/sample	777,600bytes
LAICA 100 photo/day	131,072 bytes/image	13,107,200 bytes
MAG 1/min	12/bytes	1,728 bytes
attitude 1/30s	40 bytes	115,200 bytes
temperature 1/0.5hr	1 bytes	48 bytes
total	14 mb (14,001,776 bytes) / day	

To calculate communicating time per day, the parameters listed below are needed:

Distance from LIONER to Moon: 3,736 km
 Distance from ionosphere to Moon: 1,836 km
 Distance between Earth and the Moon: ~380,000 km

Since the distance between the Earth and Moon is relative far, it can assume both of them as a point. Therefore, by a simple calculation, the maximum angle that LIONER can communicate with Earth without the interference of ionosphere (See Figure 45) is approximately 300 degree, which means communication time is about

$$\frac{300}{360} \times 86,400 = 72,000 \text{ (sec)}$$

Therefore the data amount per day for data rate = 4,800bps is:

$$72,000 \times 4,800\text{bps} = 345,600,000\text{bits} = 43.2 \text{ mb}$$

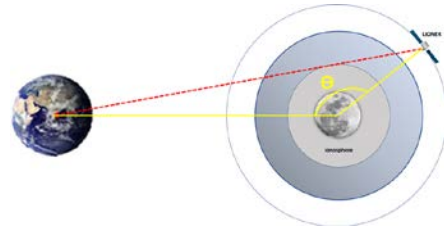


Figure 45. Maximum angle of LIONER to send signal back to Earth without ionosphere's interference.

Table 23. Link budget of the LIONER's S- and X-band communication

S-band Downlink Telemetry Budget:			X-band Downlink Telemetry Budget:		
Parameter:	Value:	Units:	Parameter:	Value:	Units:
Spacecraft:			Spacecraft:		
Spacecraft Transmitter Power Output:	2.5 watts		Spacecraft Transmitter Power Output:	14.2 watts	
In dBW:	4.0	dBW	In dBW:	11.5	dBW
In dBm:	34.0	dBm	In dBm:	41.5	dBm
Spacecraft Total Transmission Line Losses:	1.1 dB		Spacecraft Total Transmission Line Losses:	1.1 dB	
Spacecraft Antenna Gain:	10.0 dBi		Spacecraft Antenna Gain:	8.0 dBi	
Spacecraft EIRP:	12.8	dBW	Spacecraft EIRP:	18.4	dBW
Downlink Path:			Downlink Path:		
Spacecraft Antenna Pointing Loss:	0.0 dB		Spacecraft Antenna Pointing Loss:	0.0 dB	
S/C-to-Ground Antenna Polarization Loss:	3.0 dB		S/C-to-Ground Antenna Polarization Loss:	3.0 dB	
Path Loss:	211.2 dB		Path Loss:	222.7 dB	
Atmospheric Loss:	1.1 dB		Atmospheric Loss:	1.1 dB	
Ionospheric Loss:	0.8 dB		Ionospheric Loss:	0.8 dB	
Rain Loss:	0.0 dB		Rain Loss:	0.0 dB	
Isotropic Signal Level at Ground Station:	-203.3	dBW	Isotropic Signal Level at Ground Station:	-209.2	dBW
Ground Station (Eb/No Method):			Ground Station (Eb/No Method):		
----- Eb/No Method -----			----- Eb/No Method -----		
Ground Station Antenna Pointing Loss:	27.5 dB		Ground Station Antenna Pointing Loss:	27.5 dB	
Ground Station Antenna Gain:	63.6 dBi		Ground Station Antenna Gain:	74.6 dBi	
Ground Station Total Transmission Line Losses:	2.3 dB		Ground Station Total Transmission Line Losses:	2.3 dB	
Ground Station Effective Noise Temperature:	20 K		Ground Station Effective Noise Temperature:	20 K	
Ground Station Figure of Merit (G/T):	48.2 dB/K		Ground Station Figure of Merit (G/T):	59.2 dB/K	
G.S. Signal-to-Noise Power Density (S/No):	46.1	dBHz	G.S. Signal-to-Noise Power Density (S/No):	51.2	dBHz
System Desired Data Rate:	1200	bps	System Desired Data Rate:	4800	bps
In dBHz:	30.8	dBHz	In dBHz:	36.8	dBHz
Telemetry System Eb/No for the Downlink:	15.3	dB	Telemetry System Eb/No for the Downlink:	14.4	dB
Demodulation Method Selected:	Coherent FSK		Demodulation Method Selected:	QPSK	
Forward Error Correction Coding Used:	None		Forward Error Correction Coding Used:	None	
System Allowed or Specified Bit-Error-Rate:	1.0E-05		System Allowed or Specified Bit-Error-Rate:	1.0E-05	
Demodulator Implementation Loss:	1	dB	Demodulator Implementation Loss:	1	dB
Telemetry System Required Eb/No:	11.9	dB	Telemetry System Required Eb/No:	9.6	dB
Eb/No Threshold:	12.9	dB	Eb/No Threshold:	10.6	dB
System Link Margin:	2.4	dB	System Link Margin:	3.8	dB

Downlink S-band (when transmit small data amount)

Frequency = 2250MHz

Polarization= RHCP

Spacecraft transmitter power output: 2.5W

Spacecraft antenna: gain = 10dBi, beamwidth = 60°

Ground station antenna: gain = 63.6dBi, beamwidth = 0.118°

Data rate:1200bps

Demodulation type:FSK

Downlink X-band (when transmit high data amount)

Frequency = 8400MHz

Polarization= linear

Spacecraft transmitter power output: 14.2W

Spacecraft antenna: gain = 8dBi, beamwidth = 65°

Ground station antenna: gain = 74.6dBi, beamwidth = 0.066°

Data rate:4800bps

Demodulation type:QPSK

2.2.7. Payload

2.2.7.1. Ion and Electron Sensor (IES)

To this mission, aside from measuring total electron content (TEC) with RO, local measurement about concentration of ions along with electrons is also needed to determine the overall distribution of plasma. Therefore, Ion and Electron Sensor (IES) of Rosetta Plasma Consortium (RPC) in the Rosetta mission are selected as the major scientific instruments as shown in Fig. 46.

IES has capability to provide the measurements of three-dimensional distribution of plasma for the electrons with the energy from 1 to 22000 eV. Not only it has the advantages of wide measuring range, extensive angle, low mass, but it also exhibits the reliability during the Rosetta mission. These would increase the feasibility of our mission. IES determines energy of charged particles based on the deflection angles. After approaching the toroidal-shaped grid, electrons or ions will be deflected into different directions due to Lorentz force and then enter the field-free entrance aperture. Then, they will get into the ESA part of the analyzer and be assayed. Electrons within a narrow 4% energy passband will pass through the analyzers and enter microchannel plates (MCPs), where charge pulses provided by 16 discrete anodes are able to find out polar acceptance angles of particles, to determine the energy of charged particles.

The energy of electrons in the lunar ionosphere should be fell into this range. Besides, the variation of received solar wind while running interplanetary flight is smaller than that when Rosetta tracked the comet from a distance of 3AU to the perihelion. Thus, the detailed design of IES should correspond to the mission objectives. LIONER will measure the condition of plasma when it is just launched as well as the electrons constitution in the solar wind when it's between Earth and Moon. In the latter, electrons obey Maxwell-Boltzmann distribution, and the heat is several to tens of electron volts. After arriving Moon, LIONER will survey the distribution of ions and plasma around Moon and compare the result with that of RO to get exact data since RO can only provide relative values. Because the major function of IES is to measure the energy of charged particles, we will further refer to measured effects of other missions, which may provide the masses of those particles. Therefore, the composition of ions can be determined by combining both information. The selected specifications of IES are summarized in Table 24 [19].

Table 24. The specification of IES

Energy range	1 to 22000 (eV/e)
Resolution	0.04 ($\Delta E/E$)
Scan	Mode dependent
Angle range (FOV)	$90^\circ \times 360^\circ$ (2.8π sr)
Resolution (electrons)	$5^\circ \times 22.5^\circ$ (18 azimuthal \times 16 polar)
Resolution (ions)	$5^\circ \times 45^\circ$ (18 azimuthal \times 7 polar) $5^\circ \times 5^\circ$ (18 azimuthal \times 9 polar) (in solar wind direction)
Temporal resolution (3D distribution)	128 sec
Data volume per a measurement	1152 bytes
Geometric factor:total (ions)	$5 \times 10^{-4} \text{ cm}^2 \text{ sr eV}/(\text{eV counts/ion})$
Per 45° sector (ions)	$6 \times 10^{-5} \text{ cm}^2 \text{ sr eV}/(\text{eV counts/ion})$
Total (electrons)	$5 \times 10^{-4} \text{ cm}^2 \text{ sr eV}/(\text{eV counts/electron})$
Per sector (electrons)	$3 \times 10^{-5} \text{ cm}^2 \text{ sr eV}/(\text{eV counts/electron})$
Mass	1040 g
Volume	1.297 cm^3
Dimension of sensor	73 mm diameter \times 101 mm
Dimension of electronics box	139 mm \times 121 mm \times 64 mm
Power	1850 mW
Spacial Resolution	41-6806 times/km
Downlink data rate	266.6 bps

Where Energy range (eV/e) represents measuring a electron with energy range in 1 to 22K eV, resolution ($\Delta E/E$) represents that measuring interval increases as the energy in a complete data. When the 1 eV measurement is done, the next data will start at 1.04 eV, temporal resolution represents that measuring a complete data need 128 seconds, Data volume per a measurement represents how many bytes for a complete data measured by IES, and special resolution represents how many measurements can be completed in 1 km.

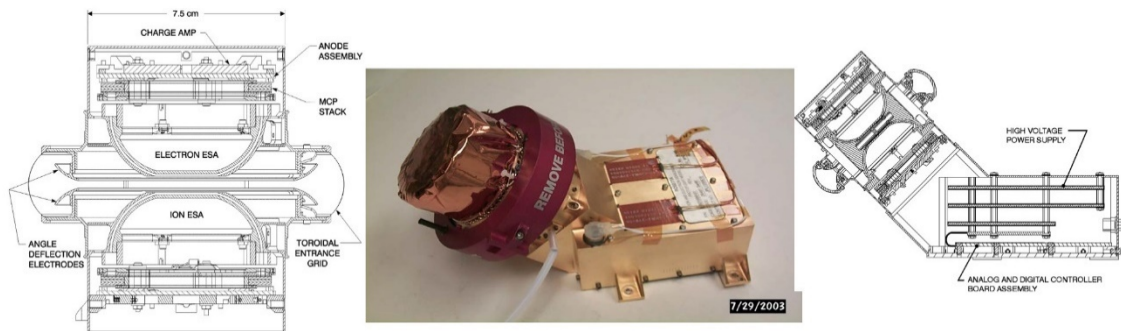


Figure 46. The Ion and Electron Sensor of the Rosetta plasma consortium (IES).

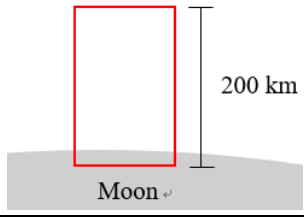


2.2.7.2. Micro camera

In order to observe the lunar corona and geocorona, LIONER is equipped with Lyman Alpha Imaging Camera (LAICA) onboard camera which has been used on PROCYON and BepiColombo mission to observe planetary exosphere and corona. The LAICA consists of three components: telescope, bandpass filter, and detector. The focal and the effective diameter of the telescope should be 250 mm and 41.5 mm, respectively. The filter should have a passband of 122 ± 10 nm. The detector component consists of five stages microchannel plates and a resistive anode. The Field Of View (FOV) will be 5.71×3.58 degrees with the angular resolution of 0.0056×0.0070 degrees which is larger than the lower limit of 2.55×10^{-4} degrees. The sensitivity should be 6.5×10^{-5} [cts/s/pix/R], and mass of the LAICA is about 2.15 kg. To ensure the LIONER can observe the geocorona from Moon and lunar corona from Earth, the view from LAICA is simulated as shown in Table 26. LIONER can also see parts of the lunar ionosphere, and corona and perform more observations at the lunar orbit. The specifications of the LAICA are summarized in Table 25. [20] [21].

Table 25. Properties of LAICA

Focal length	400mm
FOV	5.71 x 3.58 deg
Angular resolution	0.0056 x 0.0070 deg
Sensitivity	6.5×10^{-5} [cts/s/pix/R]
Effective diameter	41.5 mm
mass	2.150 kg

Table 26. Field of view of the LAICA camera

Lunar orbit → Moon	Earth orbit → Moon	Moon orbit → Earth
		

2.2.7.3. Magnetometer (MAG)

Without a strong magnetic field to deflect the solar wind, some regional anomalies could exist. These local crustal magnetic fields may be caused by meteor impacts. So, the distribution of hydrogen deposited by the solar wind is not uniform due to this unique magnetic feature. The stronger the field the denser hydrogen is allocated. Since Moon will be the first station for human being to take interplanetary expedition, it is necessary to decide optimal sites for further missions. The regions with higher hydrogen density satisfy the requirements, since hydrogen is the crucial ingredient to produce water. Therefore, it is necessary to seriously investigate the lunar magnetic field distributions.

A fluxgate MAG is equipped on the LIONER. Based on electromagnetism, a bar made of ferromagnetic metal such as iron can produce the basic notable magnetic field while wrapped by coils of wire and magnetized. The fields with opposite directions could be canceled each other by reversing the current frequently and it will present a zero field as an output value. However, the value will be shifted and the intensity of that field can be determined if an extrinsic magnetic field exists. Combining three bars situated on three different axes allows us to acquire not only its magnitude but the direction. The technology of a magnetometer has been developed through these years, so it is neither heavy nor bulky anymore.

Take the magnetometer of RPC (Rosetta Plasma Consortium) onboard Rosetta as an example, the state-of-art digital technology enables it to detect magnetic fields more precisely and simultaneously makes the entire gear to be as light as roughly 500 g as shown in Figure 47. Because all these weight, volume and precision meet our requirement, one RPC-MAG is a perfect choice for our microsat. Although a surveillance toward lunar magnetic fields was already undertaken by Lunar Prospector of NASA in 1998, it is still worth to measure the temporal variation of the lunar local magnetic field. Moreover, since LIONER is designed to be a long-term mission which means that a thorough measurement about the interaction between the solar wind and the lunar magnetic field within an entire solar cycle can be achieved.

Since the lunar magnetic field is weak, the MAG must be extended out of LIONER. The distance between the RPC-MAG and Rosetta is 1.5 meters. In comparison, an extension of approximately the length of our microsat, say, 50 cm is acceptable. Since the magnetic field around the surface on the Moon is only a few nT, the total magnetic fields generated by the satellite should be at the order of 0.1 nT. This can be achieved by arranging the instruments to reduce the overall value to appropriately several mA [22]. Table 27 summarizes the specifications of MAG.

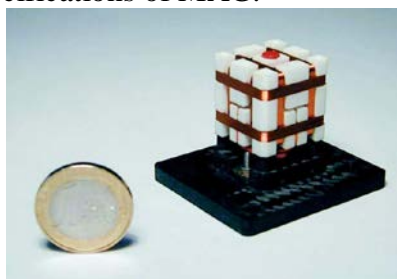


Figure 47. CSC fluxgate magnetometer.

Table 27. Properties of RPC-MAG

Dimension	25 mm × 25 mm × 25 mm
Mass	545 g (sensor, electronics and harnesses)
Power consumption	840 mW at 28 V
Range of measurement	±16384 nT
Resolution	31 pT
Temperature range	Operating: -160 ~ 120 °C Non-operating: -180 ~ 150 °C

2.2.7.4. Radio Occultation System

In order to collect radio occultation data, the LIONER will cooperate with another lunar orbit satellite, which will keep sending signal to LIONER, therefore the receiver on LIONER must be able to receive the electromagnetic signal.

There are two satellites nearby the Moon that are able to send signals, which are THEMIS/ARTEMIS and Lunar Reconnaissance Orbiter (LRO). However, because the eccentricity of THEMIS is way too large and it doesn't orbit the moon, which means it is not a good target to do the radio occultation.

LRO is a NASA robotic spacecraft currently orbiting the Moon in an eccentric polar mapping orbit launched on June 18, 2009. Mission of LRO includes selenodetic global topography, the lunar polar regions, including possible water ice deposits and the lighting environment, characterization of deep space radiation in lunar orbit, and high-resolution mapping.

There are two kinds of transmitters on LRO, one is S-band transmitter and the other is Ka-band transmitter. The transmit frequency of S-band transmitter is about 2271.2 MHz, the calculation of the link budget of LRO to LIONER can be neglected since radio occultation doesn't have to decode the signal received from LRO.

The prior criteria of choosing the radio occultation receiver of LIONER is that the receiver has to maintain the original signal and should not do any modulation after receiving it, and, the frequency range of receiving system must include 2271.2 MHz. The size of antenna is usually an important issue because it affects the efficiency of signal receiving directly. However, since LRO's transmitter is powerful enough to send data back to Earth directly, so the signal power is absolutely enough for LIONER to receive. Figure 48 shows the selected receiver for the mission, this is designed to receive GNSS signals, but still have to be modified in order to receive LRO's S-band signal. It is very easy to modify the frequency band for a receiver. For the antenna, a S-band patch antenna is selected [23]. The specifications of the receiver and antenna are summarized in Table 28 and 30.



Figure 48. NovAtel Receiver

Table 28. Properties of Receiver

Frequency range	Modified to receive 2271.2 MHz
Data Rate	Up to 100 Hz
Size	46 mm × 71 mm × 11 mm
Channels	Up to 26 Preset Channels with 20 MHz Bandwidth
Input Voltage	3.3 VDC ± 5%
Power Consumption	1.5 Watts
Mass	31 g
Size	135 mm × 50 mm × 25 mm
Operating Temperature	Operating -40 °C to +85 °C Storage -55 °C +95 °C

Table 29. Properties of antenna

Bandwidth	2.0 to 2.5 GHz
VSWR	1.3:1
Half-Power Beam Width	~ 35°
Axial Ratio	< 3 dB within 3 dB beamwidth
Mass	~ 80 g
Size	82 mm x 82 mm x 20 mm
Operating Temperature	-20°C to +50°C (operating)

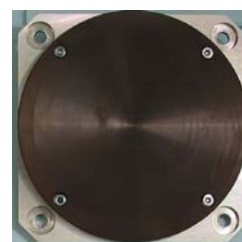


Figure 49. Antenna

2.2.7.5. SHEP Probe

LIONER is equipped with an IES to obtain information related to the charged particles from Sun. However, the impact of Sun driving the formation and variation of the lunar ionosphere depends not only on charged particles but also on solar irradiance activities.

Considered a blackbody with a surface temperature of approximately 5,800K, the Sun only radiates a small amount of the ultraviolet radiation, compared to visible light and infrared. It means that the blackbody curve representing the flux of the solar radiation falls steeply at the short wavelength region, but the real spectrum shows a controversial, and an unexpected radiation at higher energy band is figured out (See Figure 50).

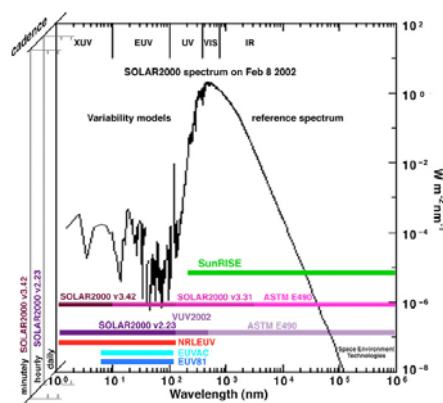


Figure 50 . The solar spectrum [24].

The high energy radiation is classified as below by their wavelength: EUV (extreme ultraviolet) , with a wavelength of 10~121 nm, XUV (soft X-ray), 0.1~10 nm, and hard X-ray, between 0.01 and 0.1nm.

Traditional UV-measuring instruments make use of photomultiplier tubes and need a high voltage supply with a certain size, mass and power consumption, and only be affordable in big satellite mission. But our predecessor cubesat “PHOENIX” in NCKU, the member of an international collaboration mission QB50 featuring in-situ measurements of the lower thermosphere on Earth, came up with an in-house instrument Solar Extreme Ultraviolet Probe (SEUV Probe). SEUV Probe measures the solar EUV radiation by the photoelectric effect, in which a photon carrying energy higher than the work function of metal will produce a photoelectron and can be measured by its photoelectric current. Therefore the SEUV Probe is an ideal instrument with the features of compact, low power consumption and light weight for the small satellite missions.

A set of the SHEP Probe (Solar High Energy Particle Probe), not only measure the solar radiation but high energy particles, consists of two types of metals with different work functions. Besides, to repel the ambient free photoelectrons, a negative bias has to be applied but more ions are attracted and forms a ion current. This current is proportional to the ambient plasma density. To distinguish it from the photoelectric current, at least a set of two probes are necessary. LIONER is equipped with three sets situated at the direction of three surfaces respectively. Therefore, the incident angle of the Sun, plasma density and solar EUV flux can be determined simultaneously.

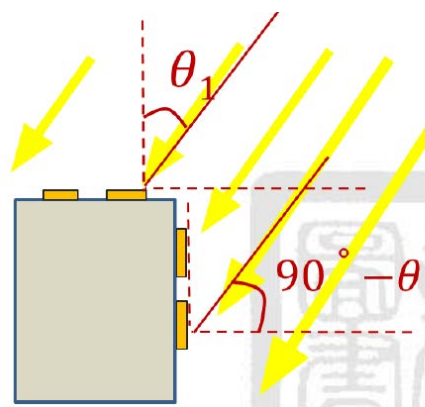


Figure 51. An illustration of parallel sunlight causing different incident angles

It is noted that the upper terrestrial atmosphere absorbs radiation with short wavelength and the EUV radiation can be only done by the instruments onboard the satellite outside the atmosphere, can not be measured by a ground observation.

Table 30. Specification of SHEP Probe

Range of measurement	<280nm
Probe	4 electrodes with radius of 1cm
Work function of metal	gold (5.1eV); tin (4.4eV)

Magnification of current	4×10^6 ; 1×, 2×, 4× and 8× extra gains
Size of PCB	95mm × 135mm
Total weight	135g (PCB, electrodes and wires)
Input voltage	3.3V and 5V
Operating temperature	0~70°C
Power consumption	0.8W (peak)

2.3. Ground segment

2.3.1. Ground station

After collecting all the data, LIONER has to send the data back to Earth. There are several antenna stations on Earth that are able to collect signals from the deep space. NASA's Deep Space Network (DSN) is one of the famous space communication facilities, it consists of three deep-space communications facilities placed approximately 120 degrees apart around the Earth, each complex consists of at least four deep space terminals equipped with ultra-sensitive receiving systems and large parabolic-dish antennas to receive signals from deep space.

There are three complexes that can be used as the ground station, they are Goldstone Deep Space Communications Complex, Madrid Deep Space Communication Complex, Canberra Deep Space Communication Complex (CDSCC). All of them are equipped with at least four deep space terminals equipped with ultra-sensitive receiving systems and large parabolic-dish antennas which have both uplink and downlink of X-band and S-band abilities, because of the location distribution of each complex, DSN should be able to complete the uplink and downlink mission whole day, so LIONER can communicate with Earth at any time when it receive the command from DSN.

2.3.2. Mission operation system

Deep Space Network will transmit uplink commands to the satellite, receive downlink scientific data and health condition from the satellite. The data and health condition will then be sent to Mission Control Center (MCC), where they will be processed, analyzed and stored. The MCC will monitor the spacecraft from launch, earth orbit, cis-lunar flight to moon orbit throughout the whole mission, analyzing scientific data and health condition, making decisions when encountering unexpected problem, as well as commanding the satellite, scheduling the scientific observations and planing the next step for the mission. The MCC will also store all mission documents for troubleshooting and future extended mission design reference. Mission operation control is to deal with the data sent from the satellite, monitor the health condition, store the data and control S-band.

2.3.3. Data distribution

Data distribution is to deal with the scientific data and health condition sent from the satellite. After being received by Deep Space Network, they are sent to the data distribution center and stored there. Data distribution center will unpack the level-0 data, executing some calibration, correction and necessary processing. Besides, data distribution center will also monitor health condition to find out potential problems and alert the staff if necessary. The final products of scientific data and health condition data will be opened to scientific community, engineering team to get more feedback of analysis and application.

2.4. Operational process

Earth orbit: Launch mode → Booting mode → Detumbling mode → propulsion mode

Cruise: cruise mode

Moon orbit: Mission mode → Communication mode

The following operation consists of three parts, including Earth orbit, Cislunar, and Lunar orbit. When in Earth orbit step, the satellite will first be in the launch mode, which satellite has been powered off before launching. After separating from the launcher, the power will be restart and thus the booting mode begin, the LIONER will start to communicate with ground station and GPS to receive Earth orbit mode commands, and then change into detumbling mode in order to successfully unfold the solar panel. At the first three Earth orbit cycles, the LIONER will check the health of every subsystems and payloads, after the examination, the ion propulsion will be turned on and begin the propulsion mode, the satellite start to propulse until the velocity is fast enough to escape from the Earth gravity.

While the satellite is in cislunar state, the ion propulsion will be turned off and move on to cruise mode. In this mode, the satellite will cruise to the moon, keep communicate with ground station, and check that every subsystem and payload works. The mission mode will be occasionally turned on to take science data such as solar wind.

After arriving the Moon, the mission mode starts, and the C&DH will begin to execute the flight software, sending commands to each science instrument. In this mode, the C&DH will continuously send commands and collect data which are going to transmit back to Earth. Table 31 is summarized the operational modes during the mission.

Table 31. Operational processes.

Spacecraft mode	Phase	Description
Booting mode	Earth orbit	Restart the communication of satellite and the ground station, unfold solar panel and power on the OBC, and start sending command to each subsystem.
Detumbling mode / Nominal mode	Earth orbit	LIONER will use momentum wheel to detumble, make sure the solar panel can be unfolded.
Propulsion mode	Earth escaping/ Insertion	The ion propulsion will be turned on and start to propulse to rise or lower the trajectory
Cruise mode	Cruise	Turn off ion propulsion, keep on the communication with Earth, check the health of every subsystem and payload. Some science instruments may be turned on in some specific time period.
Mission Mode	Moon orbit	C&DH will execute the software to send command to science instruments, collect data and then store them until the transmission.
Safe mode	Any	A mode that will be started when intend to keep the satellite alive, the non-necessary instruments are forced shut down, only main parts of the satellite will still working such as EPS, OBC, communication receiver.

3. Anticipated results

The formation of the lunar ionosphere is a mystery to scientists, and its evolution, especially under the different phases of the solar activities has not been well explored yet. Therefore, this mission is an important pioneer work to this research field.

We calculated the occultation points by the following method: First, the positions of two satellites in moon inertial coordinate system are generated by STK respectively, as shown in

Fig.52. Then the line connected two satellites and the distance between its tangential point and moon center are calculated. An radio occultation occurs if the following condition is satisfied:

$$R < r_p < 1.057 R$$

where r_p represents the shortest distance between line and moon center, R represents the radius of the Moon, roughly 1,737 km. If the distance is shorter than the Moon radius, the radio waves will be blocked by the Moon surface, being not able to be received by LIONER; if the distance is larger than $1.057 R$, i.e. the 100 km altitude where we expect the upper limit of the Moon ionosphere resides, the radio waves will not pass through the lunar ionosphere, hence it will not satisfy the occultation condition. Between the Moon surface and the upper altitude, radio signals from LRO is expected to pass through the lunar ionosphere, allowing us to measure the condition of lunar ionosphere. Using MATLAB program we calculated all possible occultation points. Moreover the point of bottom altitude are selected as representative of each profile and mark it on the plot. The calculated occultation distribution is presented as Figure 53. In one month observation, more than 1000 occultation occurred with a wide-spread distribution covering over the Moon. Similarly, replacing LRO position with the Earth in the Moon inertial coordinate system, the occultation with the radio source at the Earth's ground can be also simulated as a comparison. The occultation points in one month reduce to roughly 400, only approximately less than half of the LRO radio occultation. The distribution of occultation points with Earth is presented in Fig. 54. This result demonstrates that the occultation emitting by a moon satellite is superior than the conventional earth-based radio occultation to the exploration of the lunar ionosphere.

Recent studies shows that the earth ionosphere can be affected by activities in the lower atmosphere or lithosphere such as earthquake [Kuo et al., 2011], volcano, or tsunami. But whether the interference from the lunar lithosphere affects it ionosphere is still unknown to scientists. After receiving LRO's signal and calculating the carrier phase difference, it is expected to obtain quite amount of occultation points. Adapting the successful techniques and experience from these missions can greatly help to the naval measurement of the lunar ionosphere.

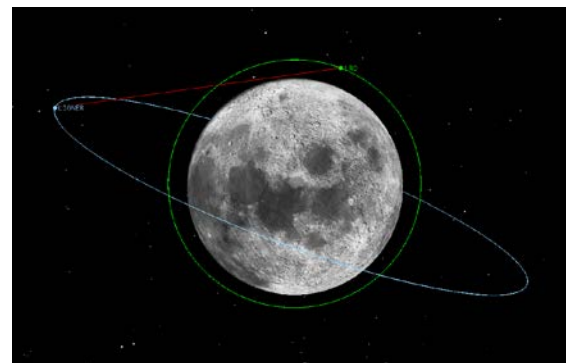


Figure 52. The line that connects LIONER and LRO (schematic).

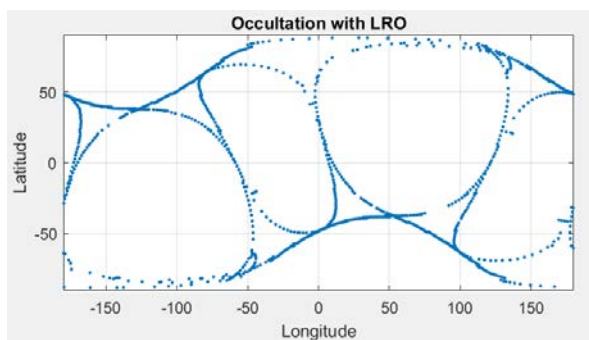


Fig 53. The distribution of occultation with LRO as a radio emitter, and 1031 points in a month is yielded.

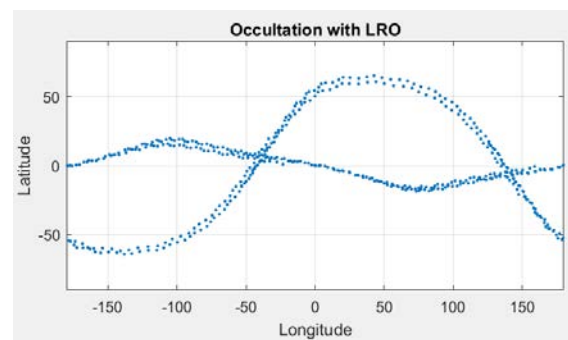


Fig 54. The distribution of occultation with earth's radio emitter, and 458 points in a month is obtained.

4. Originality and/or social effect

In planetary science, LIONER mission is the first mission to specially perform a comprehensive measurements on the lunar ionosphere using signals from existing satellites. The measurements will be able to provide a clear picture on what lunar ionosphere is comprised of and how it may have formed. As the most possible gateway for future human mission to deep space, understanding the lunar ionosphere will have a tremendous help on deep space communication from the Moon.

As an interplanetary space mission, LIONER project will be able to inspire everyone in this generation. Furthermore, as Taiwan has great experience in RO mission such as FORMOSAT-3, a RO mission to the Moon will be able to make a deeper cooperation between Taiwan and Japan on science and space engineering and will have a great chance of drawing much attention from public. Throughout the developing process of LIONER mission, students participating in it will get an impressive experience on system engineering, which will have a positive effect on them after they enter the society. LIONER will also act as a perfect platform for relating many kinds of industrials together, force many conventional industrials to upgrade and increase their competitiveness.

5. Concrete achievement methods, range and budget for manufacturing

This LIONER microsatellite will be developed by the NCKU team, associated with several institutes including Physics, Plasma and Space Science, Space Science, Aeronautics & Astronautics, Electrical Engineering department in NCKU. Table 32 summarized the budget for the LIONER mission (in US dollar).

Table 32. Esimated costs of main LIONER components

Components	Estimated cost (USD)	Components	Estimated cost (USD)
Structure	800	Thruster(RIT-10 evo)	50,000
solar cells	7,000	LAICA	300,000
battery	600	IES	300,000
PDRU(Power distribution system)	1,500	sensors	127,150
transmitter	26,000	IMU	10,000
receiver	50,000	reaction wheel	30,000
OBC	5,200	SHEPP	1,000
Total	909,250		

6. Conclusion

Among the design of the satellite, each subsystem concerns different aspect, but the mutual objective is to accomplish the scientific mission of LIONER. Those subsystems have dependence on one another and it is crucial to strike a balance for them to meet the limitations. LIONER shows us an opportunity of investigating the condition of ions in the lunar atmosphere with a microsatellite and in the future. People will get a grip of the Moon with the knowledge acquired. Besides, maybe LIONER can dedicate itself to the technology of interplanetary RO, serving as a reference for a great number of disciples who make considerable efforts just like us.

7. Reference

- [1] K M Ambili et.al., On the possibilities of the existence of molecular ions in the lunar ionosphere: a study using results from Chandrayaan-I S-Band Radio Occultation Experiment and a photochemical model, 32nd URSI GASS, Montreal, 19–26 August 2017
- [2] Jens Wickert et al., GPS Radio Occultation: Results from CHAMP, GRACE and FORMOSAT-3/COSMIC, Terr. Atmos. Ocean. Sci., Vol. 20, No. 1, 35-50, February 2009
- [3] J.Richard , A.E.Potter, Lunar Atomic Hydrogen and Its Possible Detection by Scattered Lyman Alpha Radiation, Icarus 13, 1 June 1970
- [4] The Moon Is Electric—Especially When It's Full, National Geographic, <https://www.nationalgeographic.com/science/2018/09/news-full-moon-electric-ionosphere-nasa-artemis-space/>
- [5] J.S. Halekas, A.R. Poppe, Y.Harada, J.W.Bonnell, A Tenuous Lunar Ionosphere in the Geomagnetic Tail, Geophysical Research Letters, 4 Sep, 2018
- [6] NASA-Solar activity
https://ccmc.gsfc.nasa.gov/RoR_WWW/SWREDI/2017/pesnell_SC_Pred_GSFC_SWx_Jun_2017.pdf
- [7] <https://www.ariane.group/en/equipment-and-services/satellites-and-spacecraft/rit-10-evo/>
- [8] AGI-STK-<http://help.agi.com/stk/index.htm>
- [9] Orbit of the Moon - Wiki - https://en.wikipedia.org/wiki/Orbit_of_the_Moon
- [10] A. Ruggiero , P. Pergola , S. Marcuccio , and M. Andrenucci , Low-Thrust Maneuvers for the Efficient Correction of Orbital Elements, 32nd International Electric Propulsion Conference, Wiesbaden • Germany September 11 – 15, 2011
- [11] H-IIA Launch Vehicle Upgrade Development- Upper Stage Enhancement to Extend the Lifetime of Satellites –
- [12] Ching-Lung Chiang,2004, Design and Analysis of a Pico-satellite Structures Subsystem
- [13] EFFECTIVENESS OF HONEYCOMB STRUCTURE IN MAIN BATTLE TANK DESIGN,Master of Science In: Military Vehicles Technology THESIS,Academic Year 2012-2013,HAFEEZUR RAHMAN
- [14] Honeycomb sandwich structures, Impact loads, ABAQUS. DAI YU-XIU ,HU XUAN-DE, YANG SHU-HAO,YAN CHU-HAN
- [15] Cellular solids: structure and properties from Lorna J Gibson Micheal F.Ashby
- [16] RADIATIVE VIEW FACTORS, Isidoro Martinez
- [17] Spacecraft Thermal Control Handbook Volume I: Fundamental Technologies, David G. Gilmore
- [18] Operating Strategy in PHOENIX's Attitude Determination and Control Subsystem, Sheng-Hao Wu, July, 2016
- [19] J. L. BURCHI, R. GOLDSTEIN, T. E. CRAVENS, W. C. GIBSON, R. N. LUNDIN, C. J. POLLCK, J. D. WINNINGHAM and D. T. YOUNG 27 Jun 2006, RPC-IES: THE ION AND ELECTRON SENSOR OF THE ROSETTA PLASMA CONSORTIUM
- [20] S. Kameda, S.Ikezawa, M.Sato, M.Kuwabara ,N.Osada, G.Murakami, K. Yoshioka ,I. Yoshikawa, M. Taguchi, R. Funase, S. Sugita, Y. Miyoshi, and M. Fujimoto-Published online 7 DEC 2017, Ecliptic North-South Symmetry of Hydrogen Geocorona
- [21] Optical performance of PHEBUS/EUV detector onboard BepiColombo K. Yoshioka , G. Murakami , I. Yoshikawa , J.-L. Maria , J.-F. Mariscal ,N. Rouanet d, P.-O. Mine d, E. Quemerais
- [22] MAG https://pdssbn.astro.umd.edu/catalogs/Rosetta/rpcmag_inst.cat
- [23] Chi-Yen Lin, the ionospheric radio occultation theory of FormoSat-3, 2018 ICGPSRO Student Workshop @ NCKU, Tainan
- [24] https://www.google.com.tw/search?q=solar+spectrum&source=lnms&tbm=isch&sa=X&ved=0ahUKEwiQ8Oi16OzdAhVBTLwKHSBcAUUsQ_AUIDigB&biw=1163&bih=554#imgrc=_wGqmpBiqIJseM